Specialty optical fibers for advanced sensing applications

Huanhuan Liu, Dora Juan Juan Hu, Qizhen Sun, Lei Wei, Kaiwei Li, Changrui Liao, Bozhe Li, Cong Zhao, Xinyong Dong, Yuhan Tang, Yihong Xiao, Gerd Keiser and Perry Ping Shum

---

Related articles

Advances in phase-sensitive optical time-domain reflectometry

Shuaiqi Liu, Feihong Yu, Rui Hong, Weijie Xu, Liyang Shao, Feng Wang

Opto-Electronic Advances   2022 **5**, 200078   doi: 10.29026/oea.2022.200078

Ultra-high resolution strain sensor network assisted with an LS-SVM based hysteresis model

Tao Liu, Hao Li, Tao He, Cunzheng Fan, Zhijun Yan, Deming Liu, Qizhen Sun

Opto-Electronic Advances   2021 **4**, 200037   doi: 10.29026/oea.2021.200037

Highly sensitive and fast response strain sensor based on evanescently coupled micro/nanofibers

Wen Yu, Ni Yao, Jing Pan, Wei Fang, Xiong Li, Limin Tong, Lei Zhang

Opto-Electronic Advances   2022 **5**, 210101   doi: 10.29026/oea.2022.210101

Embedded gold-plated fiber Bragg grating temperature and stress sensors encapsulated in capillary copper tube

Zhang Yanjun, Gao Haichuan, Zhang Longtu, Liu Qiang, Fu Xinghu

Opto-Electronic Engineering   2021 **48**, 200195   doi: 10.12086/oee.2021.200195

More related article in Opto-Electron Journals Group website

Specialty optical fibers for advanced sensing applications

Huanhuan Liu[1†], Dora Juan Juan Hu[2,3†], Qizhen Sun[4], Lei Wei[3],
Kaiwei Li[5], Changrui Liao[6,7], Bozhe Li[6,7], Cong Zhao[8], Xinyong Dong[9],
Yuhan Tang[9], Yihong Xiao[1], Gerd Keiser[10] and Perry Ping Shum[1,11]*

Optical fiber technology has changed the world by enabling extraordinary growth in world-wide communications and sensing. The rapid development and wide deployment of optical fiber sensors are driven by their excellent sensing performance with outstanding flexibility, functionality, and versatility. Notably, the research on specialty optical fibers is playing a critical role in enabling and proliferating the optical fiber sensing applications. This paper overviews recent developments in specialty optical fibers and their sensing applications. The specialty optical fibers are reviewed based on their innovations in special structures, special materials, and technologies to realize lab in/on a fiber. An overview of sensing applications in various fields is presented. The prospects and emerging research areas of specialty optical fibers are also discussed.

Keywords: specialty optical fibers; photonic crystal fiber; multifunctional; multi-material fibers; lab in/on fiber

Introduction

Optical fiber technology has been a key enabler in shaping worldwide high-speed communication networks and connecting different places with enhanced bandwidth, data transmission speeds, and fidelity. The development of optical fiber technology is also vital in proliferating

[1]Guangdong Key Laboratory of Integrated Optoelectronics Intellisense, Department of Electronic and Electrical Engineering, Southern University of Science and Technology, Shenzhen 518055, China; [2]Institute for Infocomm Research (I²R), Agency for Science, Technology and Research (A*STAR), 1 Fusionopolis Way, #21-01, Connexis South Tower, Singapore 138632, Singapore; [3]School of Electrical and Electronic Engineering, Nanyang Technological University, 50 Nanyang Avenue, Singapore 639798, Singapore; [4]School of Optical and Electronic Information, National Engineering Laboratory for Next Generation Internet Access System, Wuhan National Laboratory for optoelectronics, Huazhong University of Science and Technology, Wuhan 430074, China; [5]Key Laboratory of Bionic Engineering of Ministry of Education, Jilin University, Changchun 130022, China; [6]Key Laboratory of Optoelectronic Devices and Systems of Ministry of Education/Guangdong Province, College of Physics and Optoelectronic Engineering, Shenzhen University, Shenzhen 518060, China; [7]Shenzhen Key Laboratory of Photonic Devices and Sensing Systems for Internet of Things, Guangdong and Hong Kong Joint Research Centre for Optical Fibre Sensors, Shenzhen University, Shenzhen 518060, China; [8]Guangdong Laboratory of Artificial Intelligence and Digital Economy (SZ), Shenzhen 518107, China; [9]Guangdong Provincial Key Laboratory of Information Photonics Technology, School of Information Engineering, Guangdong University of Technology, Guangzhou 510006, China; [10]Department of Electrical & Computer Engineering, Boston University, Boston 02215, USA; [11]Pengcheng Laboratory, Shenzhen 518055, China.

†These authors contributed equally to this work.

*Correspondence: PP Shum, E-mail: shenp@sustech.edu.cn

Received: 29 November 2022; Accepted: 10 February 2023; Published online: 9 March 2023

sensing applications. Optical fiber sensors offer favorable advantages such as immunity to electromagnetic interference, lightweight, small size, high sensitivity, large bandwidth, reliable and robust performance, ability to withstand harsh environment, and ease in implementing multiplexed or distributed sensors. To date, optical fiber sensors have been widely used and explored for civil engineering[1–4], environmental monitoring[5–8], agricultural engineering[9,10], biomedical engineering[11–13], etc. Notably, many sensing innovations and applications are proliferated and driven by the inventions and developments of specialty optical fibers, including optical fibers with special structures, special materials, and integration with other technologies to create lab-on-fiber or lab-in-fiber devices.

This review paper aims to provide an overview of the development of specialty optical fiber technology in recent years, highlighting their achievements and future opportunities in advanced sensing applications. The first section will introduce various types of specialty optical fibers including innovations in special structures, special materials, and technology realization of the lab in/on a fiber platform. The second section will provide an application overview of specialty optical fibers in various fields, including an overview on general sensing of physical parameters, followed by wearable sensors, shape sensing, sensing in industrial applications as well as biomedical sensing. The emerging opportunities for future development of specialty optical fiber sensors will be presented in the conclusion section.

Photonic crystal fibers and optical fibers with other special structures

Photonic crystal fibers (PCFs) were invented and first fabricated using silica[14] and subsequently extended to other materials, e.g. polymer[15] and chalcogenide[16]. The air holes are developed in the core and/or cladding of the fiber structures, giving design flexibility in achieving hollow core guidance, and a wide variety of optical properties not attainable in conventional optical fibers. These novel PCFs provide new features and flexibility in engineering optical properties such as endless single-mode operation, dispersion engineering, and nonlinear properties engineering, to name a few. The PCFs family has many members with different structures. Broadly speaking, PCFs can be categorized based on their guiding mechanisms[17], such as modified index-guiding mechanism, photonic bandgap (PBG)-guiding mechanism, in-

hibited coupling-guiding mechanism, anti-resonance-guiding mechanism, twist-induced guiding mechanism, and hybrid guiding mechanism with the coexistence of both modified index-guiding and PBG-guiding mechanisms[18]. In Fig. 1, four examples of PCF structures are illustrated, including (a) hollow core PCF (bandgap effect, or antiresonance effect), (b) suspended core fiber, (c) solid core PCF, and (d) Bragg fiber.
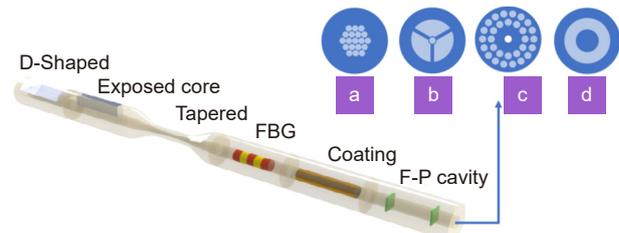

Fig. 1 | Schematic diagram of photonics crystal fibers with special structures. (**a**) Hollow core PCF (bandgap effect, or antiresonance effect). (**b**) Suspended core fiber. (**c**) Solid core PCF. (**d**) Bragg fiber.

Furthermore, PCFs have made significant achievements as a versatile platform to provide many novel functionalities and sensing application opportunities[19]. PCFs have exhibited many desirable features for physical, chemical, and biochemical sensing applications[20]. The anti-resonant fibers represent a promising route in achieving low-loss hollow core transmission and an attractive platform for developing sensing applications[21]. Hollow core PCFs are driving the development of surface-enhanced Raman scattering probes[22] and fast online Raman spectroscopy with significant performance enhancement[23]. For example, the interaction between the optical field and the analyte can be significantly enhanced through engineering the structures of the fibers, e.g. by enhancing the evanescent field to have a greater overlap with the analyte, or bringing the analyte into the hollow core or the air channels in the cladding of the fibers.

PCF-based sensors can be grouped based on their sensing structures and principles, with the possibilities of operating in combinations of several sensing principles for performance enhancements. Firstly, evanescent field based PCF sensors are developed to achieve greater sensitivity by optimizing or modifying the fiber structure to enhance the evanescent field, e.g. through air-suspended silica structures[24], tapering[25], removing partial cladding[26], etc. Secondly, the combination of grating inscription such as fiber Bragg grating and long-period grating into

PCFs have provided a powerful platform to achieve various sensing applications[27−29]. Thirdly, various interferometry configurations have been demonstrated by PCFs for physical and biomedical sensing applications, including the Fabry-Perot interferometer, Mach-Zehnder interferometer, Michelson interferometer, and Sagnac interferometer[30,31]. Fourthly, plasmonic structures are fabricated on PCFs to realize plasmonic sensing, such as thin metal films, nanowires, and nanoparticles-based PCF structures for achieving surface plasmon resonance (SPR) or localized SPR[32−34]. A representative illustration of PCF based sensor with the aforementioned sensing principles is shown in Fig. 1.

Besides PCFs, other structural modifications are bringing new possibilities to optical fiber sensors, such as specialty fibers with enhanced scattering are developed for distributed acoustic sensing[35], micro/nano fiber[36,37], fibers with whispering gallery mode microresonators[38], multicore fibers based sensor for distributed fiber sensing[39] and other sensing applications[40].

Multifunctional multimaterial fibers

Over the long history of optical fibers, the fiber material composition remained to be primarily transparent silica glass and thermoplastic polymers until about two decades ago, when material scientists from MIT put their effort into expanding the material library as well as the functionalities for thermally drawn fibers, carving out a new field called the "multimaterial multifunctional fibers"[41]. The multimaterial multifunctional fiber refers to incorporating special material into the fiber core and cladding to realize diverse functions that conventional communication optical fibers cannot attain.

The fabrication of multimaterial multifunctional fibers is similar to that of optical fibers, involving the preparation of the macroscopic preform and the thermal drawing procedure. In this sense, different materials in the same preform should have overlaps in their glass transition temperature (Tg) or melting point to ensure thermal co-drawing. For example, silica cladding can be co-drawn with semiconductors and high melting point metals; polymer cladding can be co-drawn with other polymers, chalcogenide glasses, and low melting point metals. This constraint was overcome by the convergence drawing technique in recent years, enabling the co-drawing of high melting point wires/devices with low Tg cladding materials. With a broad spectrum of functional materials (e.g., bulk glasses, polymers, metals,

semiconductors, and nanomaterials), various fiber preforms with complex geometry and material composition can be prepared by proper combined procedures of machining, thin-film rolling technique, extrusion, stack-and-draw approach, and thermal consolidation. The preform is then fed into the furnace of a fiber drawing tower and drawn into fibers with a variety of sophisticated functions. In the last 20 years, significant efforts have been put into this field, and diverse multimaterial fibers and functions such as multilayer photonic bandgap fiber[41,42], photodetecting fiber[11,43], azimuthally polarized radial fiber laser[44], piezoelectric fiber[45,46], neural probe[12], thermoelectric fiber[47,48], diode fiber[49,50], and biomedical fiber[51]. have been successfully developed. In Fig. 2, some representative works are listed to show the development history of the thermally drawn multimaterial multifunctional fibers.

(a) Multilayer photonic bandgap fibers

The multilayer photonic bandgap (PBG) fiber, reported in 2002[41], is regarded as the first proof-of-concept for the multimaterial multifunctional fiber. The fiber consisted of a hollow air core surrounded by a photonic bandgap structure established by the multiple alternating sub-micrometer-thick layers of arsenic triselenide (As_2Se_3, RI: ~2.8) and poly (ether sulphone) (PES, RI: 1.55). The transmission windows were scaled from 0.75 to 10.6 mm in wavelength by adjusting the layer thickness. Such fibers show advantages over hollow-core negative-curvature photonic crystal fibers for CO_2 laser guiding. An optoelectronic nose was also demonstrated using the multilayer PBG fiber[42].

(b) Photodetecting fibers

The first photodetecting fiber was demonstrated in 2004. The fiber consisted of a 200-μm chalcogenide semiconductor ($As_{10}Se_{50}Te_{10}Sn_5$) core and two pairs of Sn metal electrodes in contact with the core. External light could be detected by measuring the photocurrent owing to the photoconductive effect[11]. The signal-to-noise ratio could be effectively improved by decreasing the fiber photodetector's diameter[43].

(c) Azimuthally polarized radial fiber laser

The azimuthally polarized radial fiber laser is a representative work of the multimaterial multifunctional fiber. The fiber integrated a hollow photonic bandgap structure that worked as the laser cavity, the container for the
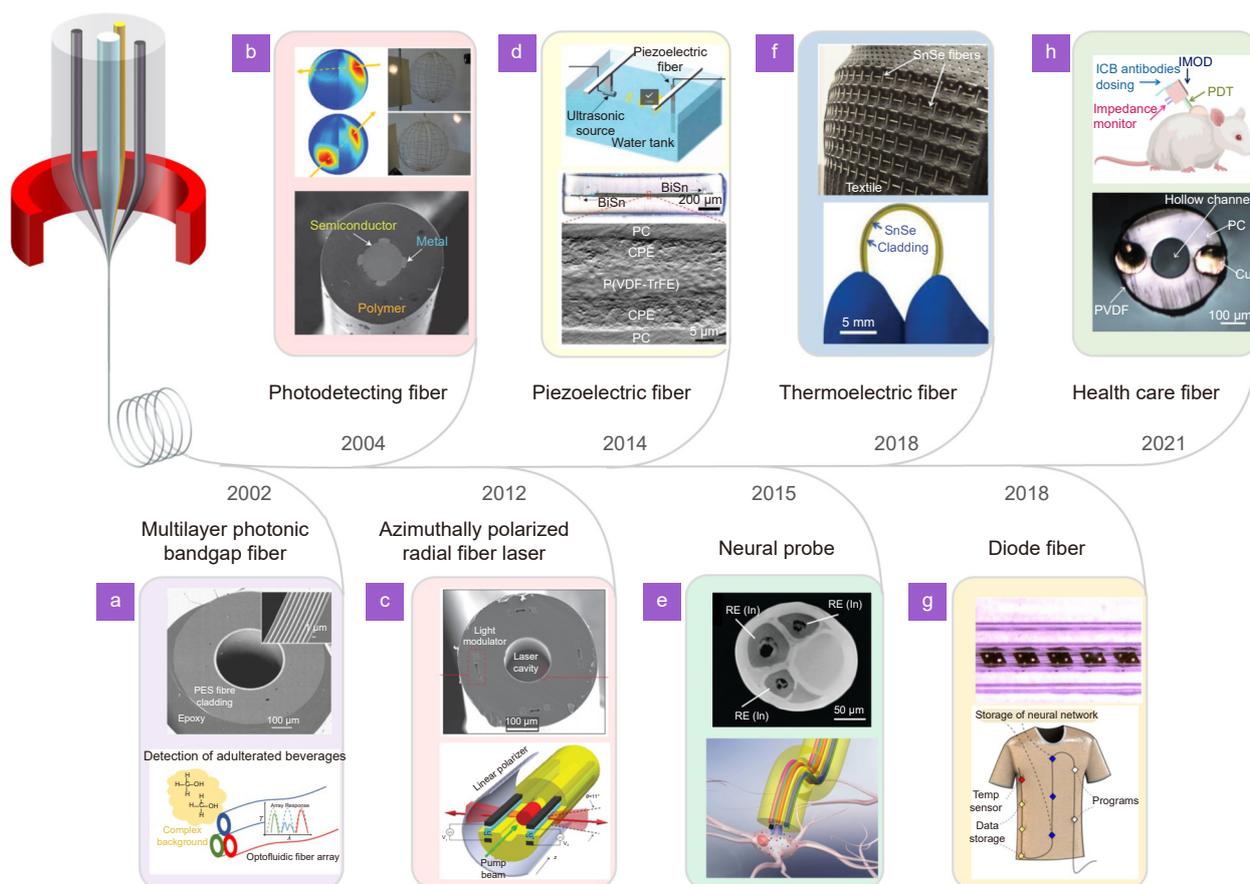
Fig. 2 | Representative works showing the development history of multimaterial multifunctional fibers. Figure reproduced with permission from: (**a**) ref.[41], Copyright © 2002 Nature Publishing Group; (**b**) ref.[11], Copyright © 2004 Nature Publishing Group; (**g**, **h**) ref.[50,51] under the terms of the Creative Commons Attribution License. The insets (**c**–**f**) are produced from our published papers in ref.[44,52,12,47], respectively.

liquid droplet gain medium, and an array of electrically contacted liquid-crystal microchannels surrounding the laser cavity. The emitted laser intensity was dynamically controlled by electrically modulating the liquid crystal window[44].

(d) Piezoelectric/thermoelectric fibers

The multimaterial piezoelectric fiber, based on the piezoelectric effect, integrated a piezoelectric P(VDF-TrFE) thin film sandwiched between two electrodes and encapsulated within a polymer cladding[45,52]. The fiber was exploited for acoustic detection from kilohertz to megahertz frequencies. A recent study further doubled the piezoelectric coefficients by loading the P(VDF-TrFE) film with piezoelectric barium titanate (BaTiO₃) ceramic particles and replacing the rigid cladding with an elastomer cladding[12], showing prospects for wearable health monitoring. Similarly, thermoelectric materials have also been successfully incorporated into multifunctional fibers to realize thermal sensing, positioning, and regulation[47,48].

(e) Neural probes

Simultaneous probing and manipulating neurons during behavioral tasks are critical to understanding neural computation in the brain and nervous system pathologies. In recent years, multimaterial multifunctional fibers have been proven to be a versatile platform for neuron probing. By integrating optical guiding paths, electrodes, and microchannels in the fiber probes, simultaneous optical stimulation, neural recording, and drug delivery in behaving mice over a long term have been realized[12].

(f) Diode fibers

Although various in-fiber optoelectronic devices have been demonstrated, their performance is still inferior to silicon chip-based ones. Alternatively, the convergence drawing technique was developed to integrate chip-based diode devices into the thermally drawn fibers. As a proof of concept, two types of in-fiber devices, including light-emitting and photodetecting p-i-n diodes, were constructed, and their potential for physiological-status monitoring and optical communication was demonstrated[49].

Furthermore, digital sensing and memory devices were integrated into one fiber and operated through a single connection at the fiber edge, providing the ability to measure and store physiological parameters and to operate neural networks for motion pattern recognition[50]. Diode fibers present intriguing opportunities in a variety of applications in wearable electronics.

(g) Biomedical fibers

The multimaterial multifunctional fibers offer a reliable new platform for implantable immune-therapeutics delivery and tumor impedance measurement. By incorporating a hollow channel, a pair of copper electrodes, and a light guiding core inside one fiber device, researchers realized local delivery of ICB antibodies and monitoring of clinical outcomes by tumor impedance measurement over a few weeks[51], demonstrating the immense potential in healthcare.

Lab in/on fiber realized by femtosecond laser induced two-photon polymerization

The intrinsic properties of optical fibers, such as ultrasmall cross-sections, ultrahigh aspect ratios, and curved surfaces, make it difficult for the conventional micro/nano fabrication strategies to be directly applied for fabricating the micro/nano structures as the key components in "lab-in/on-fiber" systems. Various micro/nano fabrication strategies, including focused ion beam (FIB), electrobeam lithography (EBL), interference lithography, femtosecond laser writing, nanoimprinting lithography, two-photon lithography, etc., have been adjusted and applied for micro/nano fabrication using substrates of optical fibers. FIB and EBL technologies could achieve fast fabrication with spatial resolution at the nanoscale, however, at the highest cost and with the limitation in mass production. Nanoimprinting lithography ensures spatial resolution at the nanoscale with the capacity of high-throughput production. Interference lithography and femtosecond laser writing are more cost-effective typically with lower spatial resolution. Recently, multi photon lithography is becoming a very intriguing technique to fabricate unique 3D micro/nano structures in/on optical fibers, which is difficult to achieve with traditional EBL and FIB methods.

　　Due to the unique advantages of two-photon polymerization (TPP) technology, such as high precision, high flexibility, and true 3D processing, it has become an innovative solution for the integration and fabrication of fiber-optic micro/nano devices. Femtosecond (fs)-laser induced TPP is basically a form of additive manufacturing based on two-photon absorption (TPA) that two photons simultaneously transfer their energy to an absorbing molecule or material[53]. Since the rate of TPA is proportional to the square of the light intensity, the polymerization can only occur at the center of the fs-laser focus point with high light intensity ($\sim$TW/cm^2)[54]. Such a nonlinear threshold effect allows the feature size of TPP to easily break the optical limit, currently down to 10 nm[55]. In recent years, a variety of micro/nanostructured devices fabricated by fs-laser induced TPP (Fig. 3), including optical waveguides, microcavities, and micro-optical elements, etc., have been developed and widely reported following the "lab-in/on-fiber" concept, in which the micro/nano structures were often located inside the fibers or on the fiber surfaces.

(a) Optical waveguides

Optical waveguides on fibers fabricated by fs-laser induced TPP enhanced the performances of "lab-in/on-fiber" devices by introducing additional polymer materials to replace the conventional quartz. One type of optical waveguides was located on the surfaces of fibers, such as fiber Bragg grating (FBG). Wang et al. in 2018 first proposed a line-by-line polymer FBG integrated on the surface of a microfiber for measuring the refractive index (*RI*) of liquids[56], as shown in Fig. 3(a). This polymer FBG showed a maximum sensitivity of $\sim$207 nm/RIU (*RI*=1.44). Subsequently, Liao et al. proposed a helical microfiber Bragg grating in 2019, as shown in Fig. 3(b). The device presented a more stable spectrum and higher mechanical robustness as a result of the increased contact area between the FBG and microfiber[57]. The FBG itself on the surface of the fiber could also enhance the mechanical strength of the device. The FBG on the fiber surface exhibited excellent *RI* responses ranging from 1.345 to 1.395. The other type of optical waveguide was located inside the fiber. Liao et al. fabricated an FBG inside a fiber with reduced width of 653 nm and increased length of 800 μm, which turned out to be a novel fiber-integrated all-optical modulator[58], as shown in Fig. 3(c). The was tested to be with a short response time of 176 ns and excellent linear modulation of −45.43 pm/mW.

(b) Optical microcavities

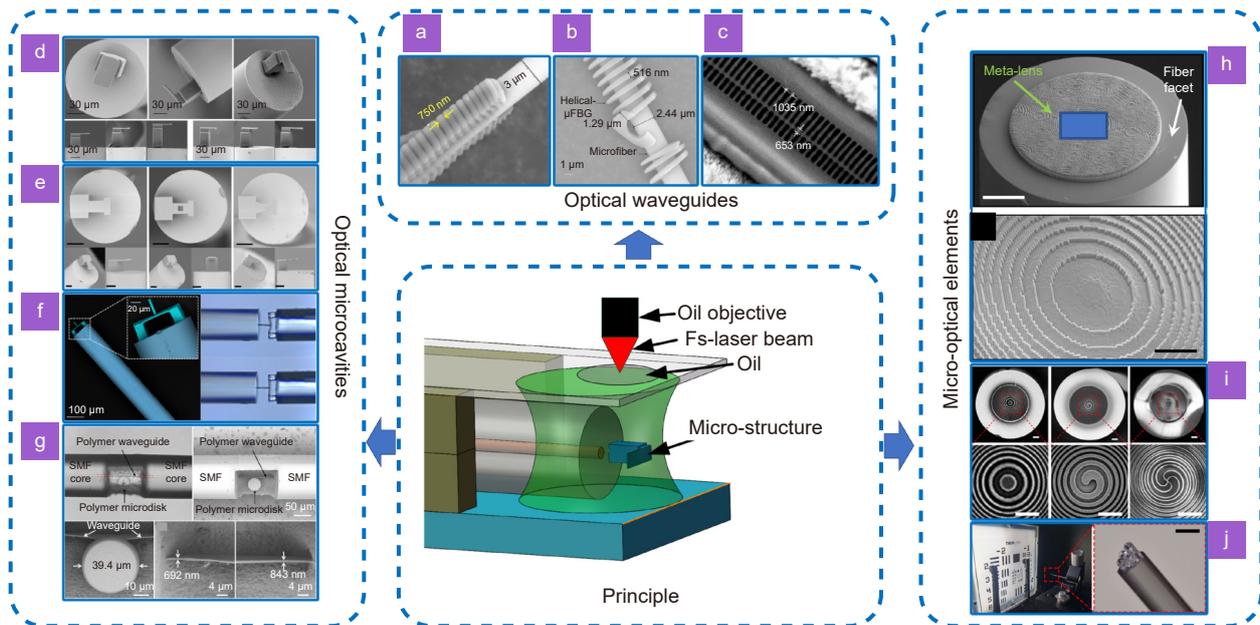Introducing optical waveguides into fibers could construct new types of highly integrated "lab-in/on-fiber"

Fig. 3 | Representative works of Lab in/on Fiber integrating with femtosecond (fs)-laser induced two-photon polymerization. (**a**) A line-by-line polymer FBG integrated on the surface of a microfiber[56]. (**b**) A helical microfiber Bragg grating[57]. (**c**) An all-optical modulator based on FBG inside a fiber[58]. (**d**) All-fiber FPI for hydrogen detection based on the fiber-tip microcantilever[59]. (**e**) The optimized fiber-tip microcantilevers[60]. (**f**) A fiber-optic microforce sensor based on fiber-tip polymer clamped-beam probe[61]. (**g**) An all-in-fiber polymer microdisk WGM resonator[62]. (**h**) Ultrathin meta-lens on the facet of modified SMF[63]. (**i**) An all-fiber beam generator based on a fiber-tip SZP[66]. (**j**) Multiple micro objective lenses on the end face of a single imaging optical fiber[67]. Figure reproduced with permission from: (**h**) ref.[63] under the terms of the Creative Commons Attribution License.

devices with high sensitivity. There are various types of microcavities, among which the Fabry-Perot interferometer (FPI) is the most widely applied one that provides excellent optical localization performance in detecting changes occurring in resonant optical paths or loss and phase changes occurring on reflective surfaces. Recently, Xiong et al. proposed an all-fiber FPI for hydrogen detection based on the fiber-tip microcantilever (Fig. 3(d))[59]. The upper surface of the microcantilever was coated with palladium (Pd) film absorbing hydrogen molecules and deforming the microcantilever, resulting in the change in the cavity length of the FPI. The device was turned to be with a sensitivity of hydrogen detection as high as −2 nm/% and a short response time of 13.5 s under 4% hydrogen. The sensitivity has been further improved by additional optimization of the microcantilever design[60], as shown in Fig. 3(e). In 2021, Zou et al. first demonstrated a fiber-optic microforce sensor using a similar fiber-tip microcantilever device, as shown in Fig. 3(f), with a sensitivity of 1.51 nm/μN and a detection limit of 54.9 nN[61]. The sensor was applied to measure Young's modulus of polydimethylsiloxane (PDMS), butterfly tentacles and human hair. This approach could open new avenues for miniaturized atomic force micro-

scopy (AFM).

Additionally, due to the high accuracy of TPP, it was also applicable for fabricating curved surfaces, such as polymer microdisks. In 2021, Ji et al. fabricated an all-in-fiber polymer microdisk whispering-gallery-mode (WGM) resonator, which was composed of a nanoscale polymer waveguide in conjunction with a polymer microdisk (Fig. 3(g))[62], with Q factor as high as 2.3 ×10³. The temperature sensitivity was 96 pm/°C in the testing range of 25 °C to 60 °C. The humidity sensitivity was also as high as 54 pm/% RH in the testing range of 30% to 90%. Such microdisk resonator could be applicable for the detection of microorganisms, bacteria and even single molecules.

(c) Micro-optical elements

The polymer material used for TPP is typically transparent with excellent light transmission capability. Since the characteristic size of TPP is smaller than the visible wavelength, it can be used to fabricate the micro-optical elements on optical fibers for optical manipulation, spatial optical coupling, beam shaping, and imaging purposes.

For optical manipulation, Malte et al. implemented ultrathin meta-lens by TPP on the facet of modified single-

mode fiber (SMF), as in Fig. 3(h), generating diffraction-limited focal spot with a record-high numerical aperture of up to $NA = 0.882$[63]. This work did not require expensive equipment, consisting only of commercial single-mode and multimode fibers. The advantage of diffractive elements over refractive lenses is their ability to produce longer working distances and ease of fabrication. High-precision capturing with high trap stiffness can facilitate single cell/particle microscopy and particle manipulation.

For spatially resolved spectroscopy, Dietrich et al. demonstrated facet-attached lens arrays fabricated by TPP. The lens arrays provided close to 100% fill-fraction along with efficiencies of up to 73% (down to 1.4 dB loss) for coupling of light from free space[64]. Subsequently, Dietrich et al. proposed *in situ* printing of facet-attached beam-shaping elements, achieving coupling efficiencies of up to 88% between edge-emitting lasers and SMFs. Printed free-form mirrors that simultaneously adapt beam shape and propagation direction were also demonstrated, along with multi-lens systems for beam expansion[65]. The concept paved the way for automated assembly of photonic multi-chip systems with unprecedented performance and versatility.

For generating a focused vortex beam, Yu et al. fabricated a compact all-fiber beam generator, as shown in Fig. 3(i), in which a spiral zone plate (SZP) was integrated on the tip of a composite fiber microstructure[66]. By adjusting the design parameters of the SZP, precise controlling of the output optical field has been achieved. The high divergence during propagation of the vortex beam was effectively overcome. The generator may have potential applications in fiber optic optical wrench, all-fiber stimulated emission depletion (STED) microscopy, and orbital angular momentum (OAM) fiber communications.

For fiber optic endoscopic imaging, Li et al., for the first time, printed multiple micro objective lenses with different fields of view on the end face of a single imaging optical fiber, as shown in Fig. 3(j), thus realizing the perfect integration of an optical fiber and objective lenses[67]. The micro-objective lenses prepared by TPP demonstrated acceptable imaging performances and thus offered a new approach for the realization of ultrathin fiber endoscopes.

Application Overview

General sensing introduction

Optical fiber sensors are widely applied to the measurement of various physical parameters due to their advantages of anti-electromagnetic interference, corrosion resistance, and small volume. New specialty optical fibers with engineered materials or specially designed structures offer new opportunities to explore novel functions and applications. Different physical parameters, for example, refractive index, temperature, strain, and magnetic, can modulate or perturb the guided light in a specialty optical fiber by means of elastic or thermos optical effects[68]. Specific applications using special optical fibers as sensors to measure refractive index, temperature, and strain are summarized below.

(a) Fiber optic refractive index sensor

Since Cooper et al.[69] proposed the first liquid refractive index fiber sensor in 1983, with the development of fiber technology, fiber refractive index sensors based on different measurement methods have been widely used[70]. According to the measurement methods, this section is divided into spectral shift, visibility, amplitude modulation and carrier phase tracking.

1) Optical fiber refractive index sensor based on spectral shift measurement

The two FBGs in series to measure temperature and the refractive index of water[71], the LPG written in pure silicon fiber[72], two large core air clad photonic crystal fibers in series[73], as shown in Fig. 4(a), a single-mode non-adiabatic tapered fiber embedded in a fiber-loop mirror[74] and ultra-wide detection range based on photonic crystal fiber surface plasmon resonance[75] are used to measure the refractive index through spectral shift measurement.

2) Optical fiber refractive index sensor based on visibility measurement

In 2008, Silva et al.[76] proposed a Fabry-Perot interferometric refractive index sensor, whose interference wavelength is derived from the reflection of short FBG and the Fresnel reflection at the far end of optical fiber. The sensitivity of 0.59 mV/RIU was obtained by measuring the amplitude of interference fringes using heterodyne technique. In 2012, Gouveia et al.[77] proposed a refractive index and temperature sensor based on Fabry-Perot interference. Based on the low reflectance Bragg grating inscribed on the panda fiber and the fiber end in contact with liquid (Fresnel reflection), the sensitivities to the refractive index and temperature can be read from the visibility of the fringe pattern the wavelength shift of the grating, respectively. In 2019, Liangtao Hou et al.[81]
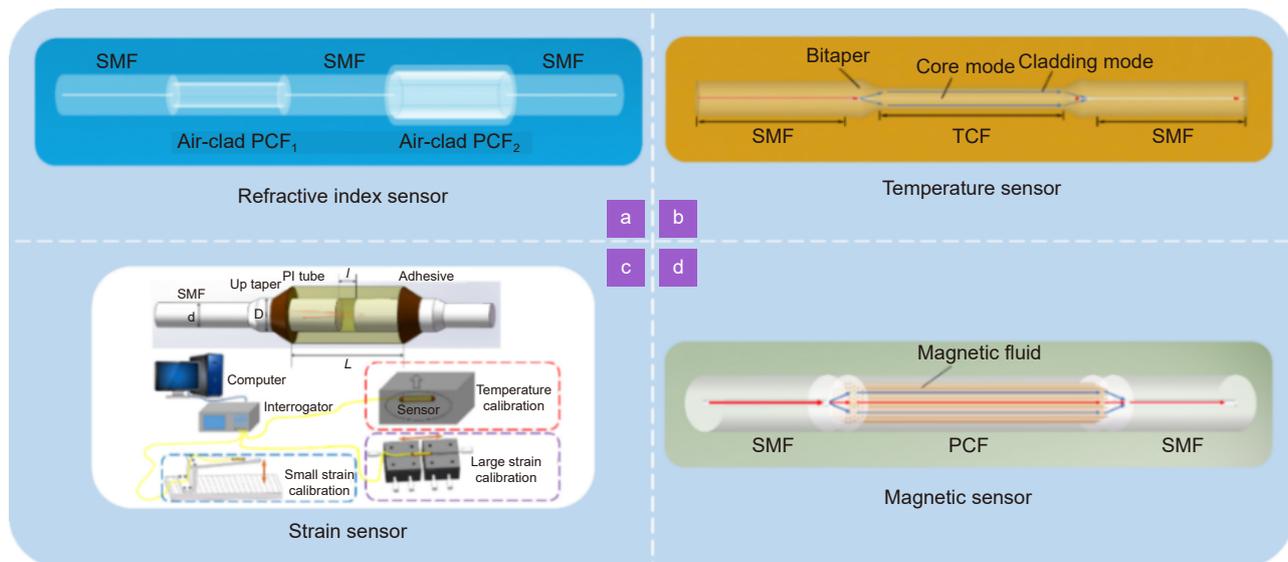
Fig. 4 | Optical fiber sensing structures for different physical parameters. (**a**) Two air-clad photonic crystal fibers with different dimensions spliced between SMF-28 single-mode fibers[73]. (**b**) A Mach-Zehnder interferometer consisting of a thin core fiber sandwiched between two waist-enlarged bitapers[78]. (**c**) The Fabry–Perot cavity stretching freely in continuous polyimide tube and its test system[79]. (**d**) Photonic crystal fiber filled with magnetic fluid sandwiched between two single mode fibers[80]. Figure reproduced with permission from: (c) ref.[79] under the terms of the Creative Commons Attribution License.

proposed a new fiber sensor based on a half-tapered single-mode-multimode-single-mode (HT-SMS) fiber structure, in which the Mach-Zehnder interferometer (MZI) was embedded in the multi-mode interferometer (MMI). According to the demodulation method of fringe visibility difference (FVD), the sensitivity of RI is 345.78 dB/RIU based on the relationship between RI and fringe visibility.

3) Optical fiber refractive index sensor based on amplitude modulation measurement

In 2006, Folate et al.[82] proposed a refractive index sensor based on phase-shifted long-period fiber grating. According to the optical power change caused by the measured object at a specific wavelength, the transmitted power modulation induced by resonance displacement was monitored, and the sensitivity of 146 µW/RIU was obtained. In 2012, Susana et al.[83] proposed a refractive index sensor based on reflection multimode interference. The sensitivity of −110 dB/RIU was obtained by measuring the refractive index through the change of the peak amplitude of the interference spectrum.

(b) Fiber optic temperature sensor

According to different operating principles, optical fiber temperature sensors in this section are divided into four categories: bend-loss, microfiber resonators, grating, interferometer and coating[84].

1) Optical fiber temperature sensor based on bend-loss

Optical loss caused by fiber bending changes with temperature. For the optical fiber temperature sensor based on step-index polymer optical fiber[85], different thermal and optical coefficients of fiber core and cladding lead to macroscopic bending loss, which affects the numerical aperture by temperature changes, and the maximum sensitivity of 1.92×10^{-3}/°C is obtained. The temperature range is 27.2–50.2 °C. Another agarose-coated macro bend optical fiber (AC-MBF) sensor[86], which is used for 2 µm relative humidity and temperature measurement, can obtain a maximum temperature sensitivity of 5.37 nm/°C and a temperature measurement range of 20−50 °C according to the variation of resonance wavelength with temperature.

2) Optical fiber temperature sensor based on Microfiber resonators

Microfibers (MFs) are unique devices formed by heating and stretching standard optical fibers to submicron sizes[87]. The temperature sensors based on microfiber are divided into two categories[87], namely resonant and nonresonant microfiber temperature sensors. The low temperature sensor based on MF-LPG is coated with a layer of silica film with a thickness of 2 µm on a conical TFLPG whose cycle increases with temperature, and its maximum temperature sensitivity is 62.9 nm/°C[88]. Pure

silica based on MFs structure is mainly used to manufacture high-temperature sensors[78], a sensor based on the principle of dual-beam interference with a maximum measuring temperature of 1000 °C. A sensitivity of 87 pm/°C was obtained by monitoring the dip at 1515.52 nm, as shown in Fig. 4(b).

3) Optical fiber temperature sensor based on grating

Fiber Bragg grating sensors for monitoring physical parameters reviewed in ref.[89] describe the progress in temperature, refractive index, and strain based on Fiber Bragg grating sensors. An FBG coated with MoS_2 with a 10 nm thick corrosion diameter of 10 μm was used for temperature sensing[90], and the temperature sensitivity from room temperature to 100 °C was measured to 95 pm/°C. An optical fiber temperature sensor using composite plating method[91], electroless nickel plating followed by electro galvanizing on FBG, can be used for low temperature sensing in the range of 280 K to 16 K. A high-temperature sensor[92] made by writing an FBG on a sapphire single crystal fiber can measure the maximum temperature up to 1900 °C. A 1-mm long FBG was written directly into microfibers splintered between standard single-mode fibers, with a maximum temperature sensitivity of 479.48 pm/°C under acetal molding.

4) Optical fiber temperature sensor based on interferometry

Optical fiber temperature sensor can use interference structures[93], such as the F-P cavity and air cavity based on thin silicon diaphragm[94] and the single-mode-no-core-single-mode fiber structure embedded in a liquid-sealed capillary[95] to measure temperature. In order to further measure the high-temperature environment[96], a FP cavity with pure sapphire structure on the end face of sapphire fiber[97] and a dual sapphire fiber based on parallel dual waveguide optical path transmission structure[98] have respectively realized the temperature measurement of 1455 °C and 1080 °C.

5) Optical fiber temperature sensor based on coating

The performance of optical fiber sensors can be improved by using coating materials[99]. The temperature sensors achieve high-sensitivity sensing by embedding in polydimethylsiloxane[100], permeating the UV-cured polymer liquid[101] or encapsulating a graphene quantum dot (GQD) solution[102].

(c) Fiber optical strain sensor

In this section, optical fiber strain sensors are divided into three categories: FBG based, multimodal interference

and Fabry-Perot cavity.

1) Optical fiber strain sensor based on FBG

The fiber Bragg grating strain sensing technology[103] such as all solid state Bragg fiber composed of concentric cladding of alternating high and low index rings[104] and etched non-photosensitive single-mode fiber with FBG[105] is reported.

2) Optical fiber strain sensor based on multimodal interference

A strain sensor based on perfluorinated graded-index polymer optical fiber is developed[106]. This type of sensor uses strain acting on part of multimode optical fiber[107] and Fresnel reflection principle of MMF remote open end[108], respectively.

3) Optical fiber strain sensor based on Fabry–Perot cavity

One for large strain and high temperature high elastic silicon oxide/polymer hybrid fiber optic sensor[79], with a continuous polyimide tube instead of the complex three layers of discontinuous glass tube, one of a pair of quartz optical fiber end face of F-P cavity can be free in the PI tube stretching, using phase tracking method, realized the 28 pm/με sensitivity, as shown in Fig. 4(c).

(d) Fiber optical magnetic sensor

Magnetic fluid is a kind of sensing element widely used in magnetic field detection[109]. According to the working principle of optical fiber magnetic field sensor, this section can be divided into three categories: grating-based sensors, interference-based sensors, and others.

1) Optical fiber magnetic sensor based on grating

Grating structures with different treatments such as phase-shifted fiber Bragg grating based on magnetic fluid infiltration[110], a tilted fiber Bragg grating coated with nanoparticle magnetic fluid[111] and ferrofluid-infiltrated micro-structured optical fiber long-period grating[112] are used as magnetic field sensors.

2) Optical fiber magnetic sensor based on interference

Magnetic field sensors based on different interference principles such as a magnetic fluid-filled FP-FBG structure[113], photonic crystal fiber filled with magnetic fluid[80], as shown in Fig. 4(d), and amplification of birefringence of magnetic fluid film by Loyt-Sagnac interferometer[114] have been developed.

3) Others

Other magnetic field sensors based on magnetic fluid include the combination of a DLUWT-based SPR fiber-optic sensor with a magnetic fluid[115], a U-bent

single-mode–multimode–single-mode fiber structure with magnetic fluid[116] and the SMF-SNS-SMF in a capillary filled with magnetic fluid[117].

Research progress related to magnetic field based on different structures and principles have been proposed, such as electromagnetic field measurement based on optical sensors[118], magneto-strictive, magneto-optical, magnetic fluid materials optical fiber current sensors, and optical fiber magnetic field sensors[119], temperature and magnetic field measurement technology based on magnetic fluids[120], optical microfiber coupler sensors[121], S-shaped fiber taper[122], optical microfibers[123], Fabry Perot interferometer fiber optic sensors[124] and core-offset structure[125].

Optical fiber wearable sensors

The spread of the Internet of Things in healthcare facilitates the transition from reactive medicine to predictive medicine. Wearable sensors are in constant development to accommodate the growing demands of healthcare devices. While, with the continuous breakthrough of flexible materials and micro-nano manufacturing processes, more and more demands have been put forward for wearable sensors, such as anti-electromagnetic interference, excellent biocompatibility, and multi-functional integration[126,127]. Thus, the further development of wearable sensing technology faces many challenges. The optical fiber sensors provide a potential alternative to overcome the limitations due to their high sensitivity, light weight, electromagnetic immunity, chemical stability, and multiplexing capabilities. To date, substantial effort in optical fiber sensors has been focused on the development of wearable healthcare monitoring, using various types such as optical fiber microstructure-based sensors[128], optical fiber interferometer-based sensors[129], and special optical fiber-based sensors[130]. In Fig. 5, representative optical fiber sensors are listed to exhibit the healthcare monitoring of the wearable application.

(a) Optical fiber microstructure-based sensors

Typical fiber microstructure-based sensors are divided into fiber Bragg grating sensors (FBG), tilted fiber Bragg grating (TFBG), and long-period fiber grating sensors (LPG)[131,132]. Fiber grating is a spatial phase grating whose refractive index is periodically modulated in the fiber core layer by utilizing the photosensitivity of the fiber material. Various physiological signals, including cardiorespiratory signals, pulse wave signals, body temperat-

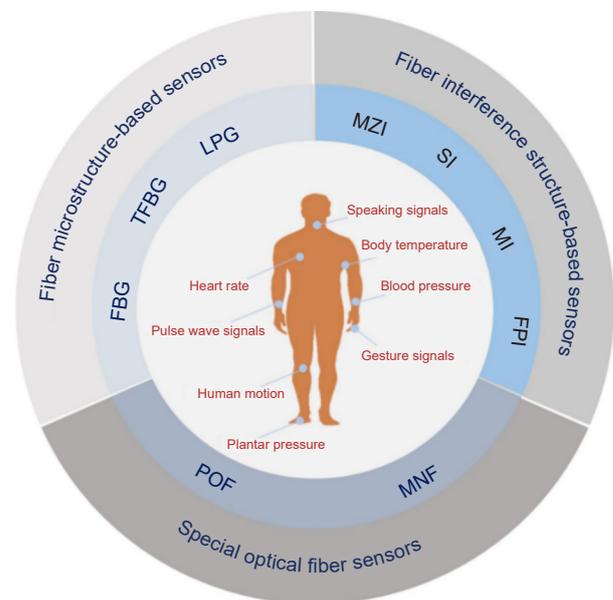ure, body posture, and plantar pressure can be monitored by demodulating the light wavelength.

Fig. 5 | Representative optical fiber sensors for wearable health monitoring.

(b) Optical fiber interferometer-based sensors

To employ a low-cost sensor system, significant effort has been devoted to developing fiber interferometer-based sensors such as Mach–Zehnder interferometer (MZI), Sagnac interferometer (SI), Michelson interferometer (MI), and Fabry-Perot interferometer (FPI)[133,134].

The MZI has a sensing arm and a reference arm. Vital signs will change the length and refractive index of the optical fiber sensing arm. For SI, it is possible to detect the phase shifts of the two beams of light transmitted in opposite directions by measuring the interference effect under the external stimulus. The structure of MI is almost identical to MZI. MI uses the reflection mode, which makes it more compact and convenient to use in experiments. FPI is the most popular phase-modulated sensor for wearable applications, and the Fabry-Perot cavity is the sensing area. It is suitable for monitoring heart rate, respiration rate, blood pressure, and body temperature due to its small size. The fiber interferometer-based sensors mentioned above offer the advantages of high sensitivity and low cost.

(c) Special optical fiber sensors

In order to promote the development of portability and integration of wearable devices, special optical fiber sensors such as polymer optical fiber (POF) sensors and

micro/nano fiber (MNF) sensors have also drawn a lot of interest in research[135,136,137], which will be significant in human-computer interaction control, human health monitoring, and movement disorders monitoring.

POF sensors based on soft and stretchable optical waveguides are usually made from hydrogels, biodegradable polymers, and elastomers. The deformation of the soft optical waveguide will cause transmission loss, leading to the intensity variation of transmitted light. Benefiting from the advantages of low Young's modulus, high flexibility, higher elastic limits, excellent biocompatibility, and wearable physiological monitoring, including body temperature, human motion, speaking, and deep breathing could be realized[138].

MNF is an optical waveguide with a diameter in the sub-wavelength order and a strong evanescent field. Un-

der external excitation, the guided modes will transit into radiation modes, leading to optical loss[139]. Skin-like wearable sensors based on microfibers have been adopted in healthcare monitoring. In addition, hardness discrimination and slippage monitoring can also be adopted by microfiber tactile sensors[140].

Optical fiber shape sensors

Optical fiber shape sensor (OFSS) is an emerging, rapidly developing technology. Due to the superiority of intrinsic safety, biocompatibility, and flexibility, OFSS has presented great progress and application prospects in areas such as biomedical treatment[141], soft robots[142], structural health monitoring[143], and aerospace engineering[144]. The common demands of these application fields are high sensitivity, high accuracy, and real-time tracking
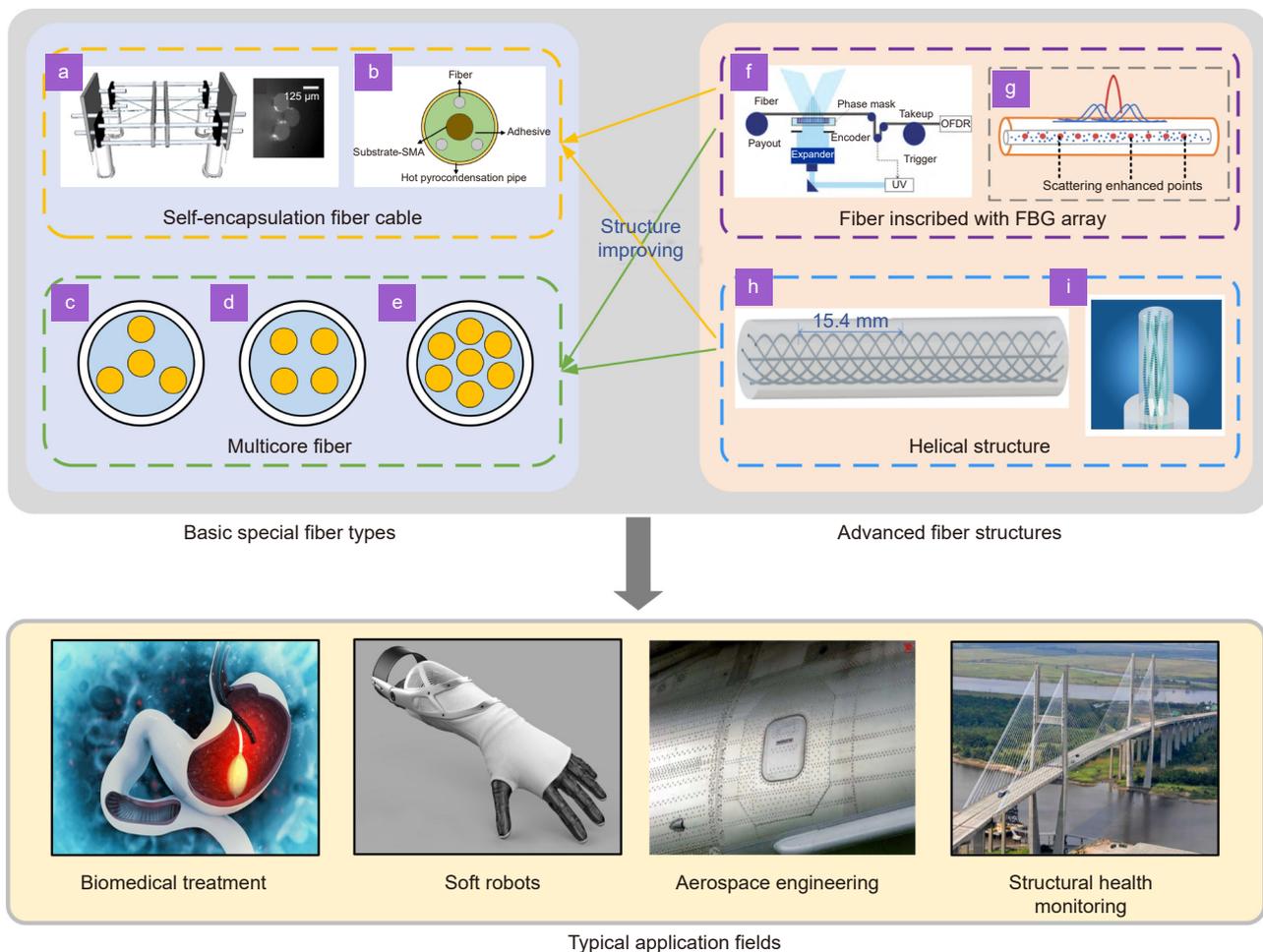

Fig. 6 | The representative special fiber types, advanced fiber structures as well as application fields exhibiting the significant development history of the optical fiber shape sensor. (**a**) A self-encapsulated fiber cable consisting of three fibers[141]. (**b**) A self-encapsulated fiber cable including three fibers and a substrate-SMA[149]. (**c–e**) Multicore fiber with core angles of 120 degrees, 90 degrees, and 60 degrees. (**f**) Setup for continuous FBG fabrication[150]. (**g**) Schematic diagram of scattering enhancement. (**h**) Helical multicore fiber with helical pitch of 15.4mm[151]. (**i**) Continuous gratings in twisted multicore fiber with UV transparent coating. Figure reproduced with permission from: (a) ref.[141], (b) ref.[149], (h) ref.[151], under the terms of the Creative Commons Attribution License; (f, i) ref.[150], Copyright © 2022 American Chemical Society.

of shape position. Currently, the measurement schemes of OFSS mainly rely on Fiber Bragg gratings (FBG)[145], optical frequency domain reflectometry (OFDR)[146], and brillouin optical time domain analyzer (BOTDA)[147]. The representative special fiber types, advanced fiber structures as well as application fields can be shown in Fig. 6.

The fiber cable of OFSS is usually composed of multiple fiber cores with the characteristic of symmetrical distribution in space, where the differential strain response between each fiber core can be employed to obtain the shape parameters along the sensing link. Then, by combing with the shape reconstruction model, the three-dimensional shape of the measured object could be deduced without visual aid[148]. From the perspective of cross-section, the relative distance and angle between each fiber core and center point should be identical. According to the packaging method of the multiple fiber cores, the special optical fibers for shape sensing can be divided into two categories, namely, self-encapsulated fiber cable and multicore optical fiber.

(a) Basic special fiber types of OFSS

Self-encapsulated fiber cable is usually composed of several ordinary single-mode fibers or Fiber Bragg grating (FBG) array fibers[141]. Through special manual bundling and packaging, the bare optical fibers are pasted around the substrate such as catheter, needle, or shape memory alloy (SMA) wire or pasted together to form a fiber cluster[149,152]. The common arrangement methods include four orthogonal or three optical fibers at an angle of 120 degrees. Due to the large core spacing of self-encapsulation fiber cable, the shape sensor has higher shape resolution and sensitivity. Nevertheless, the spatial position arrangement is greatly affected by the mechanical device and the pasting condition, so the consistency and accuracy of the sensor cannot be guaranteed.

In contrast with self-encapsulation fiber cable, multicore fiber only has one cladding, one coating as well as several cores. Among them, one core is in the center, and other cores are parallelly arranged at equal intervals of about tens of micrometers on the circumference[146,147]. For multicore fiber, the structural parameters such as core distance and core angle can be accurately controlled during the fabrication process. Therefore, the reconstruction error caused by geometric parameters is so small to be ignored. While the cost of fan-in and fan-out couplers for multicore fiber is relatively high.

(b) Advanced fiber structures for performance enhancement

It is well known that shape sensing mainly relies on the analysis for strain information, while the strain is obtained by demodulating the inherent scattering information in the fiber. Therefore, the FBG array inscribed on the optical fiber core effectively enhances the scattering magnitude of OFSS. With the improvement of femtosecond laser processing technology, it is possible to directly write fiber grating arrays on multicore fibers[150,153]. The grating spacing can reach only several millimeters, the reflectivity can be less than 1%, and the number of gratings can reach several thousand.

Furthermore, the local twist is referred to the localized circumferential angular shift of the fiber away from the neutral axis in OFSS[154]. The twist will lead to the degradation of accuracy and stability of shape sensing, and ultimately the failure of shape reconstruction. To solve this issue, the helical structure is developed and applied in both self-encapsulated fiber cable and multicore fiber.

(c) Typical applications

OFSS has shown great potential in the fields of medical treatment consisting of minimally invasive surgery[155], endovascular navigation, epidural administration, ophthalmic as well as cardiac procedures, colonoscopy, and finger gesture recognition[156]. Furthermore, OFSS can be embedded in flexible robot links and manipulator arms of continuum soft robots to realize the monitoring of motion status and position[157]. Moreover, the OFSS is also an effective real-time nondestructive monitoring method to observe and record the deformation and morphology of the structural behavior[158].

Based on the above two basic special fibers, the combination of fibers inscribed with FBG array and helical structure enable the OFSS to be more powerful, and leads to improved measurement sensitivity and reconstruction accuracy.

Applications in industry

(a) Distributed temperature sensing for industrial applications

All fiber Raman-scattering-based distributed temperature sensors (DTSs) have undergone significant improvements in technology and application over the last decades. The anti-Stokes component from spontaneous Raman scattering in fiber is temperature-sensitive and its
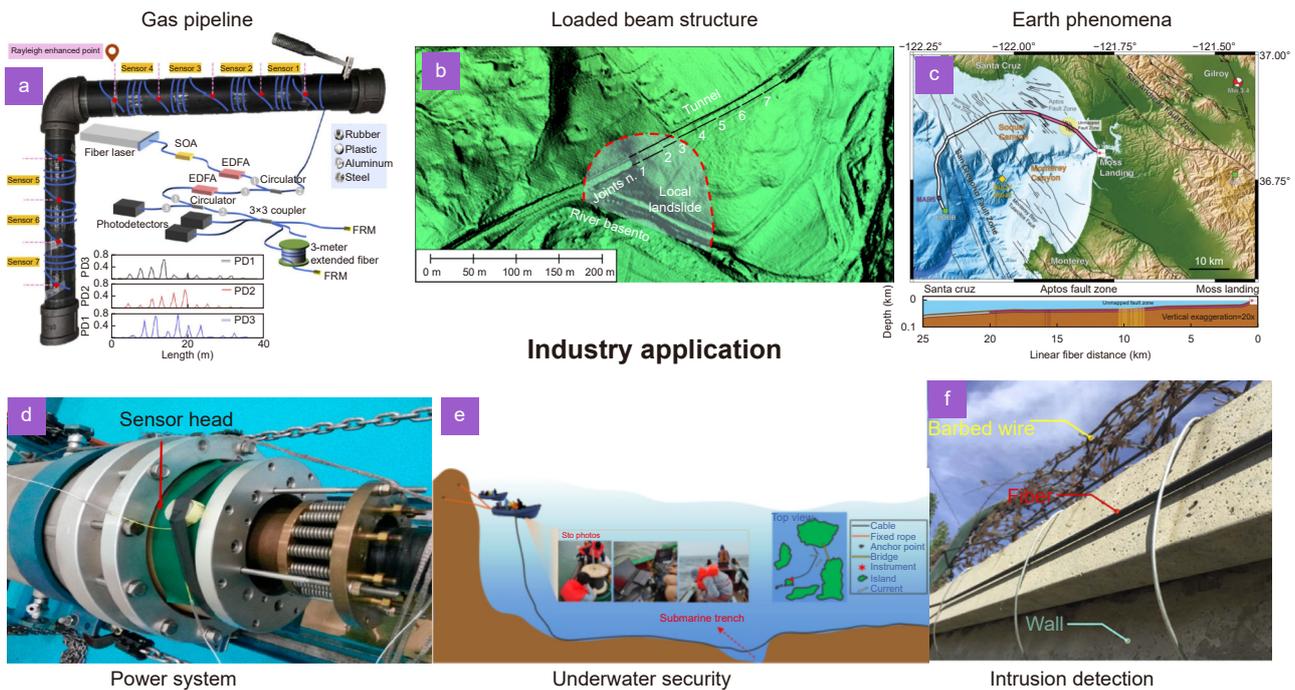
Fig. 7 | Optical fiber sensing for industry applications. (**a**) DAS in application of protecting gas pipelines against both malicious intrusions and piping degradation[6]. (**b**) Distributed fiber-optic strain sensor for long-term monitoring of a railway tunnel[166]. (**c**) DAS in application of illuminating earth phenomenon[5]. (**d**) Optical fiber sensing for detecting the partial discharge of the accessories of a high-voltage power system[7]. (**e**) Optical fiber sensing for monitoring the real-time status of the surrounding underwater environment[167]. (**f**) Optical fiber sensing for real-time intrusion threat detection on high-speed railway[168]. Figure reproduced with permission from: (a) ref.[6], (b) ref.[166], (e) ref.[167], (f) ref.[168], under the terms of the Creative Commons Attribution License; (c) ref.[5], Copyright © AAAS.

intensity can be temperature modulated. Conversely, the Stokes component is basically independent of temperature. Therefore, the utilization of Raman scattering and optical time domain reflectometry (OTDR) can achieve the spatial DTS[159]. DTS was first used to monitor wellbore temperature in oil wells, enabling continuous and long-term temperature monitoring throughout the well[160,161]. In addition, DTS system was applied to measure the temperature along the length of the cable and oil-cooled power transformer[162–164]. Fire detection is important for industrial applications. DTS was used to detect fire and localize the seat of the fire within a building with 1-m resolution[165]. DTS can be used for long-term real-time temperature monitoring in industry, but it faces the problem of short service life of optical fiber. The development of high temperature and harsh environment optical fiber has attracted increasingly more attention.

(b) Distributed temperature and strain sensor for industrial applications

Distributed Brillouin sensing was first proposed in the late 1980s to measure local attenuation along an optical fiber[169]. It has many potentialities for sensing because

Brillouin scattering is intrinsically very sensitive to temperature and the deformations experienced by the sensing fiber. Brillouin scattering results from the interaction between pumped incident light and optical phonons. The absorption or release of phonons by the pump incident light results in the Brillouin frequency shift. The Brillouin frequency shift is determined by the acoustic velocity and is a function of fiber temperature and strain. Brillouin-scattering-based distributed temperature and strain sensor (DTSS) can realize the continuous measurement of parameters in space, which has the characteristics of long-distance and high-capacity sensing. DTSS is currently the most studied system in civil structure structural health monitoring[2]. Because of the merit of the extended measurement range, DTSS has great potential in applications where large structures exist, such as dams, pipelines, tunnels, and long-span bridges[1,3]. For example, DTSS based on Brillouin sensing was used in the monitoring project of the Andes pipeline and the Italy Rimini gas pipeline to detect the geological hazard around the pipeline and monitor the pipeline deformation and leakage[170]. The challenge of Brillouin-scattering-based DTSS is the crosstalk between parameters while performing

multi-parameter measurements. In the future, new types of optical fiber and coding technology will be developed to achieve high-resolution temperature and strain sensing over long distances.

(c) Distributed acoustic sensor for industrial applications

The distributed acoustic sensor (DAS) is one of the most attractive and promising fiber sensing technologies in the recent decade. DAS is based on interference of Rayleigh backscattering and optical reflectance measurement technique, which can simultaneously detect and retrieve multiple vibrations over long distances and a high sampling rate. Compared with the well-developed DTS based on Raman scattering, the DAS based on Rayleigh scattering can detect events far from the fiber cable. And compared with the DTSS based on Brillouin scattering, the DAS can keep the coherence of the pump, so its highest strain resolution is orders of magnitude higher than the DTSS[171]. Together with its advantages like small size, immune to electromagnetic interference, and robust against harsh environment, the DAS is a promising solution in long distance applications like pipeline security, and harsh environments like oil and gas wells[172]. DAS can form a large scale and low-cost sensor array to recover the waveform of the mechanical vibration with high fidelity. The most typical industrial application is seismic wave detection. Ajo Franklin et al. used DAS deployed on a regional unlit fiber in dark fiber for broadband seismic monitoring, which showed that the optical fiber network could be effectively used for many earth science observation tasks[173]. In 2019, Lindsey et al. combined DAS with existing dark fiber in subsea cables to observe ocean and solid earth phenomena[5]. In addition to the monitoring of natural geological activities, ambient noise can also be recorded by the DAS for monitoring the Earth's near surface[174−176]. For oil and gas exploration, DAS enables signal acquisition throughout the well and is easy to deploy with lower operating costs. So the DAS processing results outperform a regional and local surface array and will become a powerful tool for long-term dynamic monitoring of oil and gas wells[177]. In industrial applications, such as intrusion detection for perimeter and fence, pipeline surveillance system, and railway security, the DAS plays a significant role because of the long working distance, linear configuration, and high sensitivity. The challenge for the DAS industrial applications is pattern recognition in event detection, while machine learning technology has great potential in the realization of high-performance pattern recognition.

(d) Various types and applications of special optical fibers

Fiber Bragg grating (FBG) is the most widely used fiber sensing technology in the industry. FBG can detect temperature, stress, strain, displacement, acceleration, and other multi-parameter information, which should be widely used in structure detection, reservoir detection and fire detection[178,179]. Polarization maintaining fiber (PMF) can ensure the linear polarization line in fiber sensing is unchanged and improve the signal-to-noise ratio. PMF is an important part of a fiber optic gyroscope, which is widely used in the inertial navigation of rockets, ships, and aircraft[180,181]. Spun HiBi fiber (SHB) is a special type of PMF, which is the main component of fiber optic current transformer and has a wide application prospect in the field of high current measurement[182]. Few-mode fiber (FMF) mitigates modal dispersion and has a high nonlinearity threshold in comparison with multi-mode fiber (MMF) and single-mode fiber (SMF). The DTS system based on FMF is expected to reach a temperature measurement distance of 50 km for online temperature monitoring of railways, power lines and long-distance oil and gas pipelines. Multi-core fiber (MCF) has flexible core numbers. It can achieve long-distance distributed bending sensing and performance enhanced distributed sensing, which may find applications in aerospace industry[39]. Photonic crystal fiber (PCF), characterized by air holes arranged along the fiber length, is regarded as a desirable platform to excite surface plasmon resonance (SPR). PCF-SPR has excellent sensing performance with controllable resonance wavelength and exceptionally high sensitivity, which can realize a new type of highly sensitive gas sensor[183,184]. This kind of gas sensor can be widely used in ocean exploration, air environment detection and human respiratory monitoring and other fields. Optical fiber sensing for industry applications can be shown in Fig. 7.

Applications in biomedical sensing

The unique physical and light-transmission properties of optical fibers make them ideal components for biomedical sensors. Various types of optical fibers are finding widespread use in biosensor instrumentation for life sciences-related clinical and research applications. Each optical fiber structure has certain advantages and limita-

tions for specific uses in different spectral bands that are of interest to various biomedical areas[185]. The following subsections describe several different biomedical sensing modalities using specialty optical fibers. These are illustrated in Fig. 8 and include (a) biorecognition sensors[186,187], (b) optical coherence tomography (OCT)[188–190], (c) surface-enhanced Raman spectroscopy (SERS)[191–193], (d) surface plasmon resonance (SPR)[194,195], and (e) Michelson interferometry[196–198]. Endoscopic methodologies are described in Section *Endoscopy* and Fig. 9.

(a) Biorecognition sensors
Biorecognition sensors are based on the principle of evanescent electromagnetic field waves in the fiber interacting with materials surrounding the fiber. Evanescent waves are not tightly bound to the fiber core but extend partially into the region surrounding the fiber. This class of evanescent wave-based sensors uses absorbance measurements to detect any variations in the concentrations of substances such as antigens that absorb a specific wavelength of light, as Fig. 8(a) shows. The absorption process of biorecognition material coating on the optical fiber results in a physical-chemical alteration that can affect the characteristic of the evanescent wave in the optical fiber. Changes in the evanescent wave are directly related to concentrations or types of biomaterials in which the sensor emerged. Applications of this methodology have been used for sensing glucose levels, pH levels, oxygen levels, and the presence of antibodies. Specialty fibers employed in this sensing technique include coated multimode and single-mode, photonic crystal fibers, and tapered fibers.

(b) Optical coherence tomography (OCT)
OCT is an optical imaging modality that can capture real-time, 3D images of biological tissues and materials in vivo and noninvasively with a 1-15-μm resolution depending on the specific OCT method used[188,189,190]. OCT is based on an interferometric optical fiber configuration
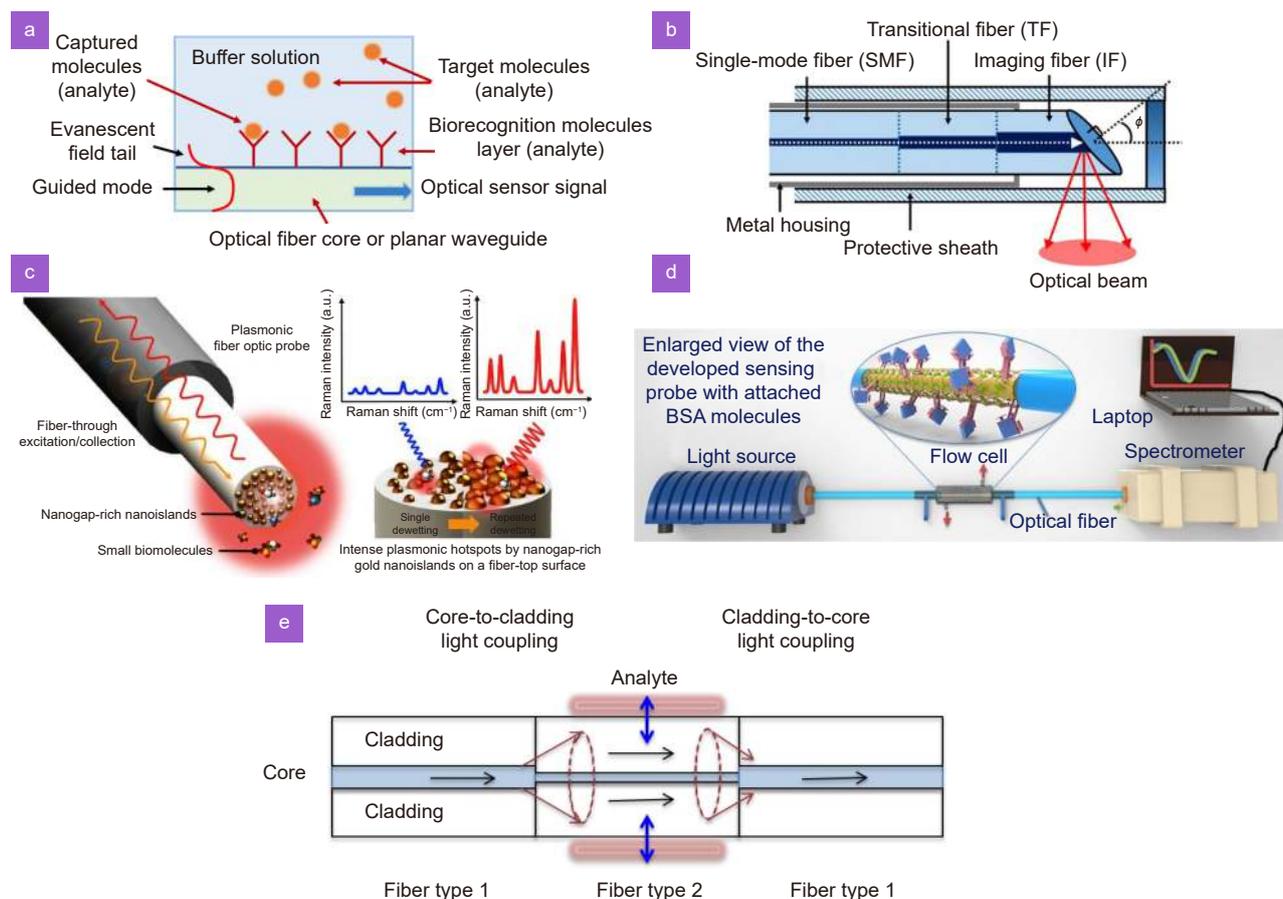
Fig. 8 | Several different biomedical sensing modalities using specialty optical fibers. These include (**a**) biorecognition sensors, (**b**) optical coherence tomography (OCT). (**c**) Surface enhanced Raman spectroscopy (SERS). (**d**) Surface plasmon resonance (SPR) and (**e**) Michelson interferometry. Figure reproduced with permission from: (b) ref.[188], (c) ref.[191], (d) ref.[199], under the terms of the Creative Commons Attribution License.
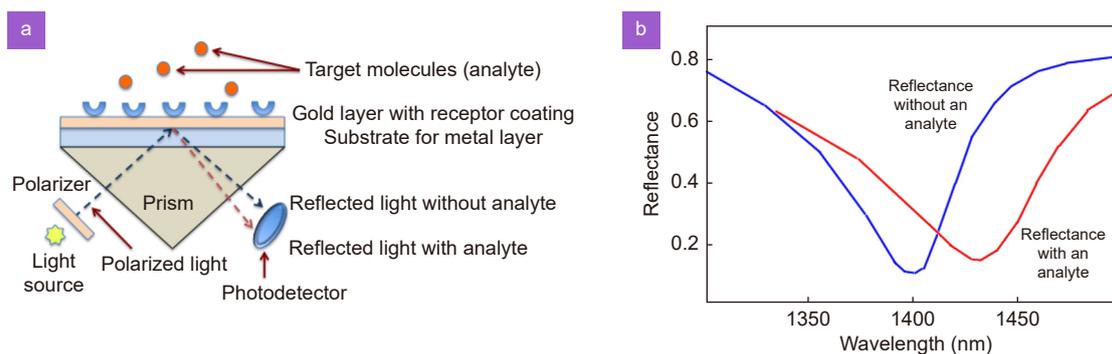
Fig. 9 | (a) Concept of a biosensor using a surface plasmon resonance effect. **(b)** Example of the shift in the surface plasmon resonance peak when there is a relative index change from captured biological samples.

and functions by measuring the intensity and time-of-flight information collected from backscattered light coming from different points within a tissue sample. Conventionally, two fibers are used in the OCT system. In this case, one of the fibers transmits illuminating light to the target specimen and the second fiber collects the reflected scattered light for reconstruction of the image by the detection system. A newer, more advanced version uses a single, multi-clad fiber (such as a double-clad fiber) where the transmission of the source light and the reflected light occurs in a single fiber. In a double-clad fiber the single-mode core transmits light to the specimen and the inner cladding collects the reflected light for the measurement instrument. In addition to the classical interferometric fiber configuration, OCT probes have also been used inside 30-gauge needles to obtain images inside the body. Such a needle probe is shown in Fig. 8(b), which uses optical fibers such as single-mode fibers, hard-clad silica fibers, photonic crystal fibers, side-emitting fibers, and double-clad collection fibers.

(c) Surface enhanced Raman spectroscopy (SERS)
SERS is based on using a large array of efficient scattering molecules, as Fig. 8(c) illustrates[191−193]. These collections of molecules can be chemically joined to metallic substrates after which they can produce distinct, optically strong spectra upon illumination by a laser. Through this process, a strong evanescent electromagnetic field is induced on the metal surface. Thereby the Raman modes of molecules that are close to the metallic surface are enhanced dramatically, because the Raman intensity is proportional to the square of the incident electromagnetic field amplitude. One analytical model to describe this effect is to consider an isolated sphere subject to a quasi-static incident electromagnetic field[192,193]. This results in the expression

$$E^2 \propto E_0^2 \left| \frac{\varepsilon_m - \varepsilon_0}{\varepsilon_m - 2\varepsilon_0} \right|^2, \tag{1}$$

here the parameter E is the electric field magnitude at the surface of the sphere, E_0 is the incident field magnitude, ε_m is the wavelength-dependent dielectric constant of the metal composing the sphere, and ε_0 is the dielectric constant of the local environment around the sphere. This relation shows that when $\varepsilon_m = -2\varepsilon_0$, which can be achieved for silver and gold at certain wavelengths in the visible and near-IR, the magnitude of the electric field at the surface of the sphere become very large.

As an alternative to attaching target molecules onto a nanoparticle roughened fiber surface, another technique is to immobilize biomarkers inside the core surface of a photonic crystal fiber. Biochemical samples can be accommodated in holes of fiber in liquid or gaseous form due to the holey nature of hollow-core photonic crystal fiber (HC-PCF), and as a result interaction between the guided light and suspected analytes is very high. Compared with the attached target molecules onto a nanoparticle fiber surface, immobilizing biomarkers inside the core surface of a HC-PCF provides better light confinement and a larger interaction length for the guided light and the analyte, resulting in an improvement in sensitivity to detect low concentrations of bio-analytes with only a few nano liter or micro liter analyte samples[200−202]. However, the band gap shifts due to refractive index change when the hollow core and air holes are filled with liquid in HC-PCF. As a result, transmitted light may not be well confined in HC-PCF, leading to larger loss. A side channel photonic crystal fiber (SC-PCF) was designed to allow liquid samples to be pumped through a side channel while light is confined and transmitted in the center solid core. By loading the SC-PCF with a mixture of gold nanoparticles and modified cells, and subsequently propagating laser light through

the central solid core, strong SERS signal can be obtained. This SERS technique achieved accurate detection of concentration of sialic acid and rapid monitoring of lipid peroxidation derived protein modification in cells[203,204].

(d) Surface plasmon resonance (SPR)

Surface plasmons are electromagnetic waves that propagate along the surface of a metallic-dielectric or a metallic-air interface and are evanescent in all other directions. The surface plasmon resonance effect produces a collective oscillation of electrons when the surface of a solid or liquid is stimulated by polarized light，as illustrated in Fig. 9(a). Because the plasmon waves travel along the surface of a thin metallic layer (on the order of several ten nanometers thickness for visible light), they are very sensitive to any changes in the boundary characteristic at the surface. For example, changes in the boundary characteristic can occur when molecules suspended in a liquid sample are adsorbed on the metal surface. These events will modify the surface plasmon mode thereby causing a shift in the resonance peak of the reflected light, as Fig. 9(b) illustrates. In order to create a more compact miniaturized SPR instrument, specially designed or modified optical fibers have been implemented to replace the much larger prism structure[194]. These fiber-based configurations include metallic coatings on a silica or plastic fiber core, tapered fibers, and photonic crystal fibers. One method that has been examined is the coating of the exposed core of a single-mode fiber with a thin layer of gold, thereby creating an SPR configuration[195]. The motivation for this type of miniature SPR probe was to work intravenously for real-time detection of circulating tumor cells in bloodstreams. By making use of the SPR effect, biosensors with a high sensitivity can be created for applications such as imaging, medical diagnostics, drug discovery, food safety analysis, and environmental monitoring. Specially designed or modified optical fibers user for SPR include metallic coatings on a silica or plastic fiber core, tapered fibers, and photonic crystal fibers.

(e) Michelson interferometry

Interferometric optical fiber sensors are based on measuring the phase difference between two superimposed light beams that have the same frequency. Commonly deployed interferometer architectures are the Mach–Zehnder, Michelson, and Sagnac interferometers[196–198]. As an example, Fig. 8(e) shows an example of Mach–Zehnder interferometer (MZI). Owing to its versatile setup configuration, an MZI is popular for diverse biosensing applications. Various degrees of sensing can be achieved in the center of the MZI by using different types of specialty fibers for fiber 2. These include multimode fibers, fibers with embedded FBGs, or photonic crystal fibers. In order to create a more compact and robust interferometer design, biosensors based on an all-fiber inline MZI scheme have been investigated. The designs include a tapered fiber configuration, a microcavity imbedded in a fiber, the use of fiber Bragg gratings, cascaded segments of different fibers, photonic crystal fibers that are selectively filled with a liquid, and nanofiber probes.

(f) Endoscopy

The field of *endoscopy* uses a photonic-based instrument containing one or more optical fibers that allow a clinician to examine the inside of a hollow organ or body cavity[205,206]. The following units make up a basic endoscope system:

• A flexible tube that encapsulates one or more optical fibers for illumination and viewing functions. The encapsulating endoscope tube also can contain miniature air, water, and suction or biopsy tubes, plus wires for tip control

• An external light source that is coupled to the optical fibers in the encapsulating tube for illuminating the organ, tissue area, or body cavity being diagnosed

• A lens system which collects reflected or fluorescing light from the diagnostic site for transmission via optical fibers to a viewer

• A viewing mechanism such as a simple eyepiece, a monitor, or a camera

New specialty optical fiber types and miniaturized cameras have helped to enable increasingly sophisticated endoscopic capabilities and have resulted in smaller, faster-performing devices. During the evolution of endoscopes, the fibers used in the instrument have included optical fiber bundles and single optical fibers such as multimode fibers, single-mode fibers, double-clad fibers, and hollow-core photonic crystal fibers.

Figure 10 shows six different configurations for using diverse optical fibers and imaging configurations inside of an endoscopic sensing head[206]. Endoscopes can be classified into side-viewing endoscopes (Fig. 10(a)) and forward-viewing endoscopes (Fig. 10(b)). A side-viewing endoscope is more suited for surveying a large area

inside of a hollow organ, while a forward-viewing endoscope is generally more suited for image guidance of biopsies or device placement. Figures 10(c) and 10(d) illustrate the use of a tethered capsule that is used to diagnose and monitor diseases in the digestive tract. The clinical procedure involves swallowing a nominally 11-mm-diameter and 30-mm long rotating viewing capsule that is tethered to an optical fiber link and captures cross-sectional microscopic images as it travels through the digestive tract. The rotation function can be performed either outside of the fiber tether (Fig. 10(c)) or by means of a micro-motor inside of the capsule (Fig. 10(d)). One method for illuminating a tissue area and for collecting the image is the use of an angle-polished ball lens fused to the end of the endoscope fiber as shown in Fig. 10(e) for side viewing. An alternative technique is to metallically coat the fiber end as is shown in Fig. 10(f) for direct end viewing.

Conclusion and prospects

Continuous research effort is devoted to pushing the technological advancement of specialty fibers for advancing and fast-growing sensing applications. The innovations in their structures, materials, and technology integration with various sensing platforms are major driving forces in developing novel specialty fibers-based sensing technologies and solutions. This review paper presents an overview of the specialty fiber technologies from three main groups: photonic crystal fibers (PCFs) and optical fibers with other special structures, multifunctional and multimaterial fibers, and lab in/on fibers. The specialty fibers have been widely used in various sensing applications in both research and real-world applications. The potential applications of fiber-based sensors can be shown in Table 1. Compared with traditional optical fiber sensors, sensor performance such as sensitivity could be significantly improved by utilizing specialty fiber-based sensors. Such demonstrations have been made through sensing of physical parameters such as refractive index, strain, temperature, and magnetic field. Wearable sensing technologies have benefitted from the development of specialty optical fibers, ranging from fiber microstructure-based sensors, fiber interferometer-based sensors, polymer optical fiber (POF) sensors, and micro/nano fiber (MNF) sensors. Optical fiber shape sensors based on special fibers and fibers with advanced structures have achieved performance enhancement and attracted growing interest in developing applications in medical treatment, soft robots, and structural behavior monitoring. Besides point sensing applications,
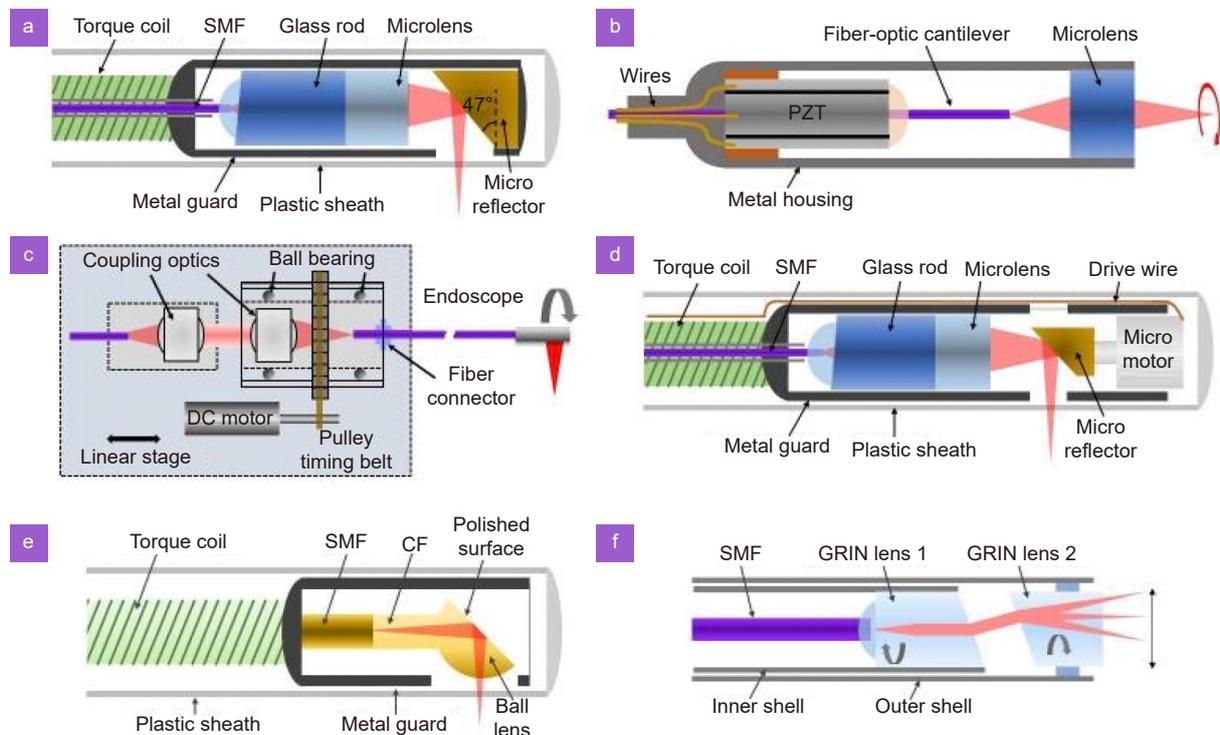

Fig. 10 | Six different configurations for using different optical fibers inside of an endoscopic sensing head. Figure reproduced with permission from: ref.[206] under the terms of the Creative Commons Attribution.

Table 1 | The potential applications of fiber-based sensors.

Technology	Potential applications	Target sensing signal	Fiber sensor type/configuration	Ref.
Wearable fiber sensors	Intelligent artificial limb	2D vector bend etc.	Seven-core fiber Bragg gratings	ref.[128]
	Heart-beat pulse rate, elasticity of the arterial wall of blood vessel	Vibration, elasticity, etc.	Tapered fiber Mach-Zehnder interferometer	ref.[129]
	Finger motion perception, Human machine interaction	Bending angle, etc.	PDMS-Teflon-Microfiber-Teflon-PDMS composite structure	ref.[130]
	Vital signs including heart rate (HR), respiration rate (RR) and body temperature	Mode interference spectrum, phase shifts, etc.	Fiber optic interferometers	ref.[133]
	Pulse wave velocity	Optical path difference, etc.	Multiplexed fiber-optic Fabry-Perot interferometric sensors	ref.[134]
	Wearable robots instrumentation, healthcare devices, human movement, plantar pressure, physiological parameters	Angles, force, temperature, humidity, etc.	Polymer optical fiber sensors	ref.[138]
	Vital signs monitoring and cardiovascular assessment	Transmitted optical power variation, etc.	Alignment-free microfiber-based sensor chip comprising an optical micro/nano fiber sensor and a flexible soft liquid sac	ref.[139]
	Robotic grasping	Force, slip, etc.	Optical microfiber	ref.[140]
Shape sensing	Biomedical treatment (e.g., invasive surgery, endovascular navigation, epidural administration, ophthalmic), soft robots, structural health monitor, aerospace engineering	Strain response, pressure, twist etc.	Self-encapsulation fiber cable composed of several ordinary single-mode fibers or Fiber Bragg grating (FBG) array fibers	ref.[141]
			Multicore fiber	ref.[131]
			Fiber grating arrays on multicore fibers	ref.[143]
			Helical structure in both self-encapsulated fiber cable and multicore fiber	ref.[144]
Industrial fiber sensing	Railway tunnel, earth phenomenon, smart grid, underwater security, intrusion detection	Raman-scattering light, Brillouin-scattering light, Rayleigh scattering light, Birefringent, etc.	Standard single mode fiber	ref.[167]
			Multi-mode fiber	ref.[207]
			Multi-core fiber	ref.[39]
			Spun HiBi fiber	ref.[182]
			Fiber Bragg grating	ref.[178] ref.[179]
			Polarization maintaining fiber	ref.[180] ref.[181]
Biomedical fiber Sensing	Biorecognition	Evanescent electromagnetic field wave, etc.	Coated multimode and single-mode, Photonic crystal fibers, Tapered fibers	ref.[187]
	Medical diagnostics, drug discovery, food safety analysis, environmental monitoring	SPR effect, etc.	Metallic coatings on a silica or plastic fiber core, tapered fibers, and photonic crystal fibers	ref.[194] ref.[195]
	In vivo 3D tissues & noninvasively imaging	Intensity and time-of-flight information, etc.	A single, multi-clad fiber (such as a double-clad fiber)	ref.[188] ref.[189] ref.[190]
	Endoscopy	Illumination Reflected or fluorescing light, etc.	Optical fiber bundles and single optical fibers such as multimode fibers, single-mode fibers, double-clad fibers, and hollow-core photonic crystal fibers	ref.[205] ref.[206]

distributed fiber sensors have been widely used for industrial applications, such as monitoring of gas pipelines, underwater security, loaded beam structure, earth phenomena, power transformer, and downhole environments. Specialty fibers are also widely used in biosensor instrumentation for life sciences related clinical, and research applications.

In addition, fs laser-based TPP technology is highly accurate and compatible with the micron- and even nano-sized features of the optical fiber itself, allowing the fabrication of microstructures with almost arbitrary designs on the fiber surface, tip, or inside the fiber. Moreover, as a direct-writing process, the substrate surface is not restricted to be flat, but can even be on the arc-shaped outer surface of the fiber. Compared with conventional UV/CO$_2$-laser based fabrication technologies, TPP not only achieves higher accuracy, but also produces microstructures with much finer surfaces which can achieve more reliable optical performances. On the other hand, beyond the resin-based photoresist, there are more types of new materials being applied in TPP, such as silica nanocomposite, gelatin-based hydrogel, etc. Other types of functionalized composite photoresist that contain magnetic nanoparticles, quantum dots, etc., are also developed for various applications. Thus, we anticipate the micro-structured fiber optic devices based on fs laser based TPP technology could gain wider application perspectives, with finer structures and more diverse functionalities.

Although many promising thermally drawn multimaterial fibers with various advanced functionalities have been achieved, the growth of multimaterial fibers is still in its early stage. More studies are desired to understand further the underlying science, material processing, structure engineering, and system integration. Here are a few exciting directions that can be investigated in the future:

1) Fabrication of semiconductor fibers with other cross-section geometries. Si and Ge fibers fabricated by far have only been cylindrical. However, other shapes of fibers are also favored in specific applications. For example, ribbon fibers or hollow-core semiconductor fibers. Ribbon fibers can be fabricated using the preform with a rectangular hollow-core, while hollow-core semiconductor fibers may be produced with a preform that has a ring-shaped hollow-core. The hollow-core semiconductor fiber can be considered as a semiconductor tube and may have interesting applications. For example,

liquid metal can be filled into the semiconductor tube to function as an electrode in an optoelectronic fiber or form an electrode array inside the semiconductor tube to achieve back-illuminated geometry.

2) Optoelectronic fibers with interdigital electrodes by the capillary breakup. For the optoelectronic fibers reported by far, two electrodes are used. For better bandwidth of the devices, more electrodes can be used to decrease the transit time of photogenerated carriers. In planar devices, the interdigital electrode is commonly used. However, in fiber geometry, deposition of the interdigital electrode is complex. Because of the capillary breakup in fibers, a thin layer of material breaks up into several fibers uniformly distributed in a ring. In this manner, a layer of conductive material arranged around the semiconductor fiber could form serval electrodes after experiencing an induced capillary breakup.

3) Fabrication of graphene nanoribbons via the cold drawing method. In the study of tearing graphene via the cold drawing method, the average width of the resulting graphene ribbon fibers is around 900 nm. Further, reducing the width of graphene ribbons to below 100 nm may open the graphene bandgap and enable many potential applications. To date, there is no report of a low-cost, simple, and fast method for producing monolayer graphene nanoribbons. Thus, it could be exciting if the cold drawing method could produce graphene nanoribbons by enhancing the adhesion of the graphene sheet and the polymer substrate.

References

1. Barrias A, Casas JR, Villalba S. A review of distributed optical fiber sensors for civil engineering applications. *Sensors* **16**, 748 (2016).
2. Lanticq V, Quiertant M, Merliot E, Delepine-Lesoille S. Brillouin sensing cable: design and experimental validation. *IEEE Sens J* **8**, 1194–1201 (2008).
3. Ravet F, Briffod F, Chin S, Rochat E, Martinez JG. Pipeline geohazard risk monitoring with optical fiber distributed sensors: experience with andean and arctic routes. In *Proceedings of the 12th International Pipeline Conference* (IPC, 2018); http://doi.org/10.1115/IPC2018-78047.
4. Zhang YJ, Gao HC, Zhang LT, Liu Q, Fu XH. Embedded gold-plated fiber Bragg grating temperature and stress sensors encapsulated in capillary copper tube. *Opto-Electron Eng* **48**, 200195 (2021).
5. Lindsey NJ, Dawe TC, Ajo-Franklin JB. Illuminating seafloor faults and ocean dynamics with dark fiber distributed acoustic sensing. *Science* **366**, 1103–1107 (2019).
6. Peng ZQ, Jian JN, Wen HQ, Gribok A, Wang MH et al. Distributed fiber sensor and machine learning data analytics for pipeline protection against extrinsic intrusions and intrinsic

corrosions. *Opt Express* **28**, 27277–27292 (2020).

7. Zhang TZ, Pang FF, Liu HH, Cheng JJ, Lv LB et al. A fiber-optic sensor for acoustic emission detection in a high voltage cable system. *Sensors* **16**, 2026 (2016).

8. Guo Y, Wu Y C, Wang J H, Zhang YF, Wang DN et al. Highly sensitive gas-pressure sensor based on paralleled optical fiber Fabry-Perot interferometers. *Opto-Electron Eng* **49**, 210420 (2022).

9. Allsop TDP, Neal R, Wang CL, Nagel DA, Hine AV et al. An ultra-sensitive aptasensor on optical fibre for the direct detection of bisphenol A. *Biosens Bioelectron* **135**, 102–110 (2019).

10. Goh LS, Kumekawa N, Watanabe K, Shinomiya N. Hetero-core spliced optical fiber SPR sensor system for soil gravity water monitoring in agricultural environments. *Comput Electron Agric* **101**, 110–117 (2014).

11. Bayindir M, Sorin F, Abouraddy AF, Viens J, Hart SD et al. Metal-insulator-semiconductor optoelectronic fibres. *Nature* **431**, 826–829 (2004).

12. Canales A, Jia XT, Froriep UP, Koppes RA, Tringides CM et al. Multifunctional fibers for simultaneous optical, electrical and chemical interrogation of neural circuits *in vivo*. *Nat Biotechnol* **33**, 277–284 (2015).

13. Guan BO, Jin L, Ma J, Liang YZ, Bai X. Flexible fiber-laser ultrasound sensor for multiscale photoacoustic imaging. *Opto-Electron Adv* **4**, 200081 (2021).

14. Knight JC, Birks TA, Russell PSJ, Atkin DM. All-silica single-mode optical fiber with photonic crystal cladding: errata. *Opt Lett* **22**, 484–485 (1997).

15. van Eijkelenborg MA, Large MCJ, Argyros A, Zagari J, Manos S et al. Microstructured polymer optical fibre. *Opt Express* **9**, 319–327 (2001).

16. Toupin P, Brilland L, Renversez G, Troles J. All-solid all-chalcogenide microstructured optical fiber. *Opt Express* **21**, 14643–14648 (2013).

17. Markos C, Travers JC, Abdolvand A, Eggleton BJ, Bang O. Hybrid photonic-crystal fiber. *Rev Mod Phys* **89**, 045003 (2017).

18. Hu DJJ, Xu ZL, Shum PP. Review on photonic crystal fibers with hybrid guiding mechanisms. *IEEE Access* **7**, 67469–67482 (2019).

19. Russell PSJ. Photonic-crystal fibers. *J Lightwave Technol* **24**, 4729–4749 (2006).

20. Calcerrada M, García-Ruiz C, González-Herráez M. Chemical and biochemical sensing applications of microstructured optical fiber-based systems. *Laser Photon Rev* **9**, 604–627 (2015).

21. Ni WJ, Yang CY, Luo YY, Xia R, Lu P et al. Recent advancement of anti-resonant hollow-core fibers for sensing applications. *Photonics* **8**, 128 (2021).

22. Yang X, Shi C, Newhouse R, Zhang JZ, Gu C. Hollow-core photonic crystal fibers for surface-enhanced raman scattering probes. *Int J Opt* **2011**, 754610 (2011).

23. Ding HN, Hu DJJ, Yu XT, Liu XX, Zhu YF et al. Review on all-fiber online raman sensor with hollow core microstructured optical fiber. *Photonics* **9**, 134 (2022).

24. Jensen JB, Pedersen LH, Hoiby PE, Nielsen LB, Hansen TP et al. Photonic crystal fiber based evanescent-wave sensor for detection of biomolecules in aqueous solutions. *Opt Lett* **29**, 1974–1976 (2004).

25. Taha BA, Ali N, Sapiee NM, Fadhel MM, Mat Yeh RM et al. Comprehensive review tapered optical fiber configurations for sensing application: trend and challenges. *Biosensors* **11**, 253 (2021).

26. Zhuo LQ, Tang JY, Zhu WG, Zheng HD, Guan HY et al. Side polished fiber: a versatile platform for compact fiber devices and sensors. *Photonic Sens* **13**, 230120 (2023).

27. Liao CR, Zhu F, Lin CP. Photonic crystal fiber-based grating sensors. In *Handbook of Optical Fibers,* Peng GD eds. 2201–2229 (Springer, Singapore, 2019).

28. Rindorf L, Bang O. Sensitivity of photonic crystal fiber grating sensors: biosensing, refractive index, strain, and temperature sensing. *J Opt Soc Am B* **25**, 310–324 (2008).

29. Eggleton BJ, Westbrook PS, Windeler RS, Spälter S, Strasser TA. Grating resonances in air-silica microstructured optical fibers. *Opt Lett* **24**, 1460–1462 (1999).

30. Liu ZY, Tam HY, Htein L, Tse MLV, Lu C. Microstructured optical fiber sensors. *J Lightwave Technol* **35**, 3425–3439 (2017).

31. Hu DJJ, Wong RYN, Shum PP. Photonic crystal fiber-based interferometric sensors. In *Selected Topics on Optical Fiber Technologies and Applications,* Xu F, Mou CB eds. 21–41 (IntechOpen, 2018).

32. Rifat AA, Ahmed R, Yetisen AK, Butt H, Sabouri A et al. Photonic crystal fiber based plasmonic sensors. *Sens Actuator B:Chem* **243**, 311–325 (2017).

33. Hu DJJ, Ho HP. Recent advances in plasmonic photonic crystal fibers: design, fabrication and applications. *Adv Opt Photonics* **9**, 257–314 (2017).

34. Caucheteur C, Guo T, Albert J. Review of plasmonic fiber optic biochemical sensors: improving the limit of detection. *Anal Bioanal Chem* **407**, 3883–3897 (2015).

35. Sun YX, Li H, Fan CZ, Yan BQ, Chen JF et al. Review of a specialty fiber for distributed acoustic sensing technology. *Photonics* **9**, 277 (2022).

36. Lou JY, Wang YP, Tong LM. Microfiber optical sensors: a review. *Sensors* **14**, 5823–5844 (2014).

37. Cai DW, Xie Y, Guo X, Wang P, Tong LM. Chalcogenide glass microfibers for mid-infrared optics. *Photonics* **8**, 497 (2021).

38. Zheng Y, Wu ZF, Shum PP, Xu ZL, Keiser G et al. Sensing and lasing applications of whispering gallery mode microresonators. *Opto-Electron Adv* **1**, 180015 (2018).

39. Zhao ZY, Tang M, Lu C. Distributed multicore fiber sensors. *Opto-Electron Adv* **3**, 190024 (2020).

40. Zhao ZY, Dang YL, Tang M. Advances in multicore fiber grating sensors. *Photonics* **9**, 381 (2022).

41. Temelkuran B, Hart SD, Benoit G, Joannopoulos JD, Fink Y. Wavelength-scalable hollow optical fibres with large photonic bandgaps for CO_2 laser transmission. *Nature* **420**, 650–653 (2002).

42. Yildirim A, Ozturk FE, Bayindir M. Smelling in chemically complex environments: an optofluidic bragg fiber array for differentiation of methanol adulterated beverages. *Anal Chem* **85**, 6384–6391 (2013).

43. Abouraddy AF, Shapira O, Bayindir M, Arnold J, Sorin F et al. Large-scale optical-field measurements with geometric fibre constructs. *Nat Mater* **5**, 532–536 (2006).

44. Stolyarov AM, Wei L, Shapira O, Sorin F, Chua SL et al. Micro-fluidic directional emission control of an azimuthally polarized radial fibre laser. *Nat Photonics* **6**, 229–233 (2012).

45. Chocat N, Lestoquoy G, Wang Z, Rodgers DM, Joannopoulos JD et al. Piezoelectric fibers for conformal acoustics. *Adv Mater* **24**, 5327–5332 (2012).

46. Yan W, Noel G, Loke G, Meiklejohn E, Khudiyev T et al. Single fibre enables acoustic fabrics via nanometre-scale vibrations. *Nature* **603**, 616–623 (2022).

47. Zhang T, Li KW, Zhang J, Chen M, Wang Z et al. High-performance, flexible, and ultralong crystalline thermoelectric fibers. *Nano Energy* **41**, 35–42 (2017).

48. Zhang J, Zhang T, Zhang H, Wang ZX, Li C et al. Single-crystal snse thermoelectric fibers via laser-induced directional crystallization: from 1D fibers to multidimensional fabrics. *Adv Mater* **32**, 2002702 (2020).

49. Rein M, Favrod VD, Hou C, Khudiyev T, Stolyarov A et al. Diode fibres for fabric-based optical communications. *Nature* **560**, 214–218 (2018).

50. Loke G, Khudiyev T, Wang B, Fu S, Payra S et al. Digital electronics in fibres enable fabric-based machine-learning inference. *Nat Commun* **12**, 3317 (2021).

51. Chin AL, Jiang S, Jang E, Niu LQ, Li LW et al. Implantable optical fibers for immunotherapeutics delivery and tumor impedance measurement. *Nat Commun* **12**, 5138 (2021).

52. Wang S, Zhang T, Li KW, Ma SY Chen M et al. Flexible piezoelectric fibers for acoustic sensing and positioning. *Adv Electron Mater* **3**, 1600449 (2017).

53. Cumpston BH, Ananthavel SP, Barlow S, Dyer DL, Ehrlich JE et al. Two-photon polymerization initiators for three-dimensional optical data storage and microfabrication. *Nature* **398**, 51–54 (1999).

54. Farsari M, Chichkov BN. Two-photon fabrication. *Nat Photonics* **3**, 450–452 (2009).

55. Zhang YL, Guo L, Wei S, He YY, Xia H et al. Direct imprinting of microcircuits on graphene oxides film by femtosecond laser reduction. *Nano Today* **5**, 15–20 (2010).

56. Wang J, Lin CP, Liao CR, Gan ZS, Li ZY et al. Bragg resonance in microfiber realized by two-photon polymerization. *Opt Express* **26**, 3732–3737 (2018).

57. Liao CR, Yang KM, Wang J, Bai ZY, Gan ZS et al. Helical microfiber bragg grating printed by femtosecond laser for refractive index sensing. *IEEE Photonics Technol Lett* **31**, 971–974 (2019).

58. Liao CR, Li C, Wang C, Wang Y, He J et al. High-speed all-optical modulator based on a polymer nanofiber bragg grating printed by femtosecond laser. *ACS Appl Mater Interfaces* **12**, 1465–1473 (2020).

59. Xiong C, Zhou JT, Liao CR, Zhu M, Wang Y et al. Fiber-tip polymer microcantilever for fast and highly sensitive hydrogen measurement. *ACS Appl Mater Interfaces* **12**, 33163–33172 (2020).

60. Liao CR, Xiong C, Zhao JL, Zou MQ, Zhao YY et al. Design and realization of 3D printed fiber-tip microcantilever probes applied to hydrogen sensing. *Light Adv Manuf* **3**, 3–13 (2022).

61. Zou MQ, Liao CR, Liu S, Xiong C, Zhao C et al. Fiber-tip polymer clamped-beam probe for high-sensitivity nanoforce measurements. *Light Sci Appl* **10**, 171 (2021).

62. Ji P, Zhu M, Liao CR, Zhao C, Yang KM et al. In-fiber polymer microdisk resonator and its sensing applications of temperature and humidity. *ACS Appl Mater Interfaces* **13**, 48119–48126 (2021).

63. Plidschun M, Ren HR, Kim J, Förster R, Maier SA et al. Ultrahigh numerical aperture meta-fibre for flexible optical trapping. *Light Sci Appl* **10**, 57 (2021).

64. Dietrich PI, Harris RJ, Blaicher M, Corrigan MK, Morris TJ et al. Printed freeform lens arrays on multi-core fibers for highly efficient coupling in astrophotonic systems. *Opt Express* **25**, 18288–18295 (2017).

65. Dietrich PI, Blaicher M, Reuter I, Billah M, Hoose T et al. In situ 3D nanoprinting of free-form coupling elements for hybrid photonic integration. *Nat Photonics* **12**, 241 (2018).

66. Yu J, Wang YP, Yang W, Bai ZY, Xie ZW et al. All-fiber focused beam generator integrated on an optical fiber tip. *Appl Phys Lett* **116**, 241102 (2020).

67. Li BZ, Liao CR, Cai ZH, Zhou J, Zhao C et al. Femtosecond laser 3D printed micro objective lens for ultrathin fiber endoscope. *Fundam Res* (2022).

68. Villatoro J, Zubia J. Ultrasensitive sensors based on specialty optical fibres. In *Proceedings of 2016 18th International Conference on Transparent Optical Networks* (IEEE, 2016); http://doi.org/10.1109/ICTON.2016.7550360.

69. Cooper PR. Refractive-Index measurements of liquids used in conjunction with optical fibers. *Appl Opt* **22**, 3070–3072 (1983).

70. Jorge PAS, Silva SO, Gouveia C, Tafulo P, Coelho L et al. Fiber optic-based refractive index sensing at INESC porto. *Sensors* **12**, 8371–8389 (2012).

71. Pereira DA, Frazao O, Santos JL. Fiber Bragg grating sensing system for simultaneous measurement of salinity and temperature. *Opt Eng* **43**, 299–304 (2004).

72. Rego GM, Santos JL, Salgado MH. Refractive index measurement with long-period gratings arc-induced in pure-silica-core fibres. *Opt Commun* **259**, 598–602 (2006).

73. Silva S, Santos JL, Malcata FX, Kobelke J, Schuster K et al. Optical refractometer based on large-core air-clad photonic crystal fibers. *Opt Lett* **36**, 852–854 (2011).

74. Zibaii MI, Frazao O, Latifi H, Jorge PAS. Controlling the sensitivity of refractive index measurement using a tapered fiber loop mirror. *IEEE Photonics Technol Lett* **23**, 1219–1221 (2011).

75. Wang GY, Lu Y, Duan LC, Yao JQ. A refractive index sensor based on PCF with ultra-wide detection range. *IEEE J Sel Top Quantum Electron* **27**, 5600108 (2021).

76. Silva SFO, Frazão O, Caldas P, Santos JL, Araujo FM et al. Optical fiber refractometer based on a Fabry-Pérot interferometer. *Opt Eng* **47**, 054403 (2008).

77. Gouveia C, Jorge PAS, Baptista JM, Frazao O. Fabry–Pérot cavity based on a high-birefringent fiber bragg grating for refractive index and temperature measurement. *IEEE Sens J* **12**, 17–21 (2012).

78. Zhao N, Lin QJ, Jiang ZD, Yao K, Tian B et al. High temperature high sensitivity multipoint sensing system based on three cascade mach–zehnder interferometers. *Sensors* **18**, 2688 (2018).

79. Yi L, Changyuan Y. Highly stretchable hybrid silica/polymer optical fiber sensors for large-strain and high-temperature application. *Opt Express* **27**, 20107–20116 (2019).

80. Li XG, Zhou X, Zhao Y, Lv RQ. Multi-modes interferometer for magnetic field and temperature measurement using Photonic crystal fiber filled with magnetic fluid. *Opt Fiber Technol* **41**, 1–6 (2018).

81. Hou LT, Zhang XD, Yang JR, Kang J, Ran LL. Simultaneous measurement of refractive index and temperature based on half-tapered SMS fiber structure with fringe-visibility difference demodulation method. *Opt Commun* **433**, 252–255 (2019).

82. Falate R, Frazão O, Rego G, Fabris JL, Santos JL. Refractometric sensor based on a phase-shifted long-period fiber

grating. *Appl Opt* **45**, 5066–5072 (2006).

83. Silva S, Frazão O, Santos JL, Malcata FX. A reflective optical fiber refractometer based on multimode interference. *Sens Actuators B:Chem* **161**, 88–92 (2012).

84. Soge AO. Polymer optical fibre temperature sensors - A review. *Asian J Res Rev Phys* **3**, 19–37 (2020).

85. Moraleda AT, García CV, Zaballa JZ, Arrue J. A temperature sensor based on a polymer optical fiber macro-bend. *Sensors* **13**, 13076–13089 (2013).

86. Chen WJ, Chen ZH, Zhang Y, Li H, Lian YH. Agarose coated macro-bend fiber sensor for relative humidity and temperature measurement at 2μm. *Opt Fiber Technol* **50**, 118–124 (2019).

87. Talataisong W, Ismaeel R, Brambilla G. A review of microfiber-based temperature sensors. *Sensors* **18**, 461 (2018).

88. Lee CL, Weng ZY, Lin CJ, Lin YY. Leakage coupling of ultra-sensitive periodical silica thin-film long-period grating coated on tapered fiber. *Opt Lett* **35**, 4172–4174 (2010).

89. Sahota JK, Gupta N, Dhawan D. Fiber Bragg grating sensors for monitoring of physical parameters: a comprehensive review. *Opt Eng* **59**, 060901 (2020).

90. Sridhar S, Sebastian S, Asokan S. Temperature sensor based on multi-layer MoS_2 coated etched fiber Bragg grating. *Appl Opt* **58**, 535–539 (2019).

91. Sugino M, Ogata M, Mizuno K, Hasegawa H. Development of zinc coating methods on fiber bragg grating temperature sensors. *IEEE Trans Appl Supercond* **26**, 9000606 (2016).

92. Ahmed F, Jun MBG. Microfiber bragg grating sandwiched between standard optical fibers for enhanced temperature sensing. *IEEE Photonics Technol Lett* **28**, 685–688 (2016).

93. Roriz P, Silva S, Frazão O, Novais S. Optical fiber temperature sensors and their biomedical applications. *Sensors* **20**, 2113 (2020).

94. Liu TG, Yin JD, Jiang JF, Liu K, Wang S et al. Differential-pressure-based fiber-optic temperature sensor using Fabry-Perot interferometry. *Opt Lett* **40**, 1049–1052 (2015).

95. Hu PB, Chen ZM, Yang M, Yang JY, Zhong C. Highly sensitive liquid-sealed multimode fiber interferometric temperature sensor. *Sens Actuators A:Phys* **223**, 114–118 (2015).

96. Liu TG, Yu X, Wang S, Jiang JF, Liu K. Fiber-optic fabry-perot sensing technology in high-temperature environments: an review. *Laser Optoelectron Prog* **58**, 1306002 (2021).

97. Yang S, Feng ZA, Jia XT, Pickrell G, Ng W et al. Miniature all-sapphire single-crystal fiber fabry-perot sensor fabricated by femtosecond laser micro-machining and CO_2 laser welding. In *Proceedings of 2020 Conference on Lasers and Electro-Optics* 1–2 (IEEE, 2020).

98. Yu X, Wang S, Jiang JF, Liu K, Wu ZY et al. Self-filtering high-resolution dual-sapphire-fiber-based high-temperature sensor. *J Lightwave Technol* **37**, 1408–1414 (2019).

99. Li CX, Yang WL, Wang M, Yu XY, Fan JY et al. A review of coating materials used to improve the performance of optical fiber sensors. *Sensors* **20**, 4215 (2020).

100. Hernández-Romano I, Monzón-Hernández D, Moreno-Hernández C, Moreno-Hernandez D, Villatoro J. Highly sensitive temperature sensor based on a polymer-coated microfiber interferometer. *IEEE Photonics Technol Lett* **27**, 2591–2594 (2015).

101. Zhang FC, Xu XZ, He J, Du B, Wang YP. Highly sensitive temperature sensor based on a polymer-infiltrated Mach-Zehnder interferometer created in graded index fiber. *Opt Lett* **44**, 2466–2469 (2019).

102. Zhao Y, Tong RJ, Chen MQ, Xia F. Fluorescence temperature sensor based on GQDs solution encapsulated in hollow core fiber. *IEEE Photonics Technol Lett* **29**, 1544–1547 (2017).

103. Campanella CE, Cuccovillo A, Campanella C, Yurt A, Passaro VMN. Fibre bragg grating based strain sensors: review of technology and applications. *Sensors* **18**, 3115 (2018).

104. Liu NL, Li YH, Wang Y, Wang HY, Liang WB et al. Bending insensitive sensors for strain and temperature measurements with Bragg gratings in Bragg fibers. *Opt Express* **19**, 13880–13891 (2011).

105. Ferreira MS, Bierlich J, Becker M, Schuster K, Santos JL et al. Ultra-high sensitive strain sensor based on post-processed optical fiber bragg grating. *Fibers* **2**, 142–149 (2014).

106. Soge AO, Dairo OF, Sanyaolu ME, Kareem SO. Recent developments in polymer optical fiber strain sensors: a short review. *J Opt* **50**, 299–313 (2021).

107. Mizuno Y, Hagiwara S, Kawa T, Lee H, Nakamura K. Displacement sensing based on modal interference in polymer optical fibers with partially applied strain. *Jpn J Appl Phys* **57**, 058002 (2018).

108. Kawa T, Numata G, Lee H, Hayashi N, Mizuno Y et al. Single-end-access strain and temperature sensing based on multimodal interference in polymer optical fibers. *IEICE Electron Express* **14**, 20161239 (2017).

109. Alberto N, Domingues MF, Marques C, André P, Antunes P. Optical fiber magnetic field sensors based on magnetic fluid: a review. *Sensors* **18**, 4325 (2018).

110. Bao LF, Dong XY, Zhang SQ, Shen CY, Shum PP. Magnetic field sensor based on magnetic fluid-infiltrated phase-shifted fiber bragg grating. *IEEE Sens J* **18**, 4008–4012 (2018).

111. Yang DX, Du L, Xu ZQ, Jiang YJ, Xu J et al. Magnetic field sensing based on tilted fiber Bragg grating coated with nanoparticle magnetic fluid. *Appl Phys Lett* **104**, 061903 (2014).

112. Miao YP, Zhang KL, Liu B, Lin W, Zhang H et al. Ferrofluid-infiltrated microstructured optical fiber long-period grating. *IEEE Photonics Technol Lett* **25**, 306–309 (2013).

113. Xia J, Wang FY, Luo H, Wang Q, Xiong SD. A magnetic field sensor based on a magnetic fluid-filled FP-FBG structure. *Sensors* **16**, 620 (2016).

114. Zu P, Chan CC, Koh GW, Lew WS, Jin YX et al. Enhancement of the sensitivity of magneto-optical fiber sensor by magnifying the birefringence of magnetic fluid film with Loyt-Sagnac interferometer. *Sens Actuators B:Chem* **191**, 19–23 (2014).

115. Rodríguez-Schwendtner E, Díaz-Herrera N, Navarrete MC, González-Cano A, Esteban Ó. Plasmonic sensor based on tapered optical fibers and magnetic fluids for measuring magnetic fields. *Sens Actuators A:Phys* **264**, 58–62 (2017).

116. Zhang RX, Liu TG, Han Q, Chen YF, Li L. U-bent single-mode–multimode–single-mode fiber optic magnetic field sensor based on magnetic fluid. *Appl Phys Express* **7**, 072501 (2014).

117. Rao J, Pu SL, Yao TJ, Su DL. Ultrasensitive magnetic field sensing based on refractive-index-matched coupling. *Sensors* **17**, 1590 (2017).

118. Peng J, Jia SH, Bian JM, Zhang S, Liu JB et al. Recent progress on electromagnetic field measurement based on optical sensors. *Sensors* **19**, 2860 (2019).

119. Liu C, Shen T, Wu HB, Feng Y, Chen JJ. Applications of

magneto-strictive, magneto-optical, magnetic fluid materials in optical fiber current sensors and optical fiber magnetic field sensors: a review. *Opt Fiber Technol* **65**, 102634 (2021).

120. Li YQ, Wen FF, Wang SL. Research progress of temperature and magnetic field dual-parameter measurement technology based on magnetic fluids. *Laser Optoelectron Prog* **59**, 0500003 (2022).

121. Dai ML, Chen ZM, Zhao YF, Gandhi MSA, Li Q et al. State-of-the-art optical microfiber coupler sensors for physical and biochemical sensing applications. *Biosensors* **10**, 179 (2020).

122. Yu YS, Zhu YQ, Zhao Y, Pan PX. Research progress on s fiber taper. *Acta Photon Sin* **48**, 1148009 (2019).

123. Yan SC, Xu F. A review on optical microfibers in fluidic applications. *J Micromech Microeng* **27**, 093001 (2017).

124. Islam R, Ali MM, Lai MH, Lim KS, Ahmad H. Chronology of fabry-perot interferometer fiber-optic sensors and their applications: a review. *Sensors* **14**, 7451–7488 (2014).

125. Niu HW, Zhang S, Chen WH, Liu Y, Li X et al. Optical fiber sensors based on core-offset structure: a review. *IEEE Sens J* **21**, 22388–22401 (2021).

126. Gao QW, Zhang JJ, Xie ZW, Omisore O, Zhang JY et al. Highly stretchable sensors for wearable biomedical applications. *J Mater Sci* **54**, 5187–5223 (2019).

127. Leal-Junior A, Avellar L, Biazi V, Soares MS, Frizera A et al. Multifunctional flexible optical waveguide sensor: on the bioinspiration for ultrasensitive sensors development. *Opto-Electron Adv* **5**, 210098 (2022).

128. Hou MX, Yang KM, He J, Xu XZ, Ju S et al. Two-dimensional vector bending sensor based on seven-core fiber Bragg gratings. *Opt Express* **26**, 23770–23781 (2018).

129. Chen NK, Hsieh YH, Lee YK. Tapered fiber Mach-Zehnder interferometers for vibration and elasticity sensing applications. *Opt Express* **21**, 11209–11214 (2013).

130. Li YP, Tan SJ, Yang LY, Li LY, Fang F et al. Optical microfiber neuron for finger motion perception. *Adv Fiber Mater* **4**, 226–234 (2022).

131. Zhao YH, Wang CL, Yin GL, Jiang BQ, Zhou KM et al. Simultaneous directional curvature and temperature sensor based on a tilted few-mode fiber Bragg grating. *Appl Opt* **57**, 1671–1678 (2018).

132. Jin YX, Chan CC, Dong XY, Zhang YF. Temperature-independent bending sensor with tilted fiber Bragg grating interacting with multimode fiber. *Opt Commun* **282**, 3905–3907 (2009).

133. Lyu WM, Chen SY, Tan FZ, Yu CY. Vital signs monitoring based on interferometric fiber optic sensors. *Photonics* **9**, 50 (2022).

134. Ushakov NA, Markvart AA, Liokumovich LB. Pulse wave velocity measurement with multiplexed fiber optic fabry-perot interferometric sensors. *IEEE Sens J* **20**, 11302–11312 (2020).

135. Guo JJ, Yang CX, Dai QH, Kong LJ. Soft and stretchable polymeric optical waveguide-based sensors for wearable and biomedical applications. *Sensors* **19**, 3771 (2019).

136. Pan J, Zhang Z, Jiang CP, Zhang L, Tong LM. A multifunctional skin-like wearable optical sensor based on an optical micro-/nanofibre. *Nanoscale* **12**, 17538–17544 (2020).

137. Yu W, Yao N, Pan J, Fang W, Li X et al. Highly sensitive and fast response strain sensor based on evanescently coupled micro/nanofibers. *Opto-Electron Adv* **5**, 210101 (2022).

138. Leal-Junior AG, Diaz CAR, Avellar LM, Pontes MJ, Marques C et al. Polymer optical fiber sensors in healthcare applications: a comprehensive review. *Sensors* **19**, 3156 (2019).

139. Li LY, Liu YF, Song CY, Sheng SF, Yang LY et al. Wearable alignment-free microfiber-based sensor chip for precise vital signs monitoring and cardiovascular assessment. *Adv Fiber Mater* **4**, 475–486 (2022).

140. Jiang CP, Zhang Z, Pan J, Wang YC, Zhang L et al. Finger-skin-inspired flexible optical sensor for force sensing and slip detection in robotic grasping. *Adv Mater Technol* **6**, 2100285 (2021).

141. Parent F, Loranger S, Mandal KK, Iezzi VL, Lapointe J et al. Enhancement of accuracy in shape sensing of surgical needles using optical frequency domain reflectometry in optical fibers. *Biomed Opt Express* **8**, 2210–2221 (2017).

142. Wang HS, Zhang RX, Chen WD, Liang XW, Pfeifer R. Shape detection algorithm for soft manipulator based on fiber bragg gratings. *IEEE/ASME Trans Mechatron* **21**, 2977–2982 (2016).

143. Villatoro J, van Newkirk A, Antonio-Lopez E, Zubia J, Schüelzgen A et al. Ultrasensitive vector bending sensor based on multicore optical fiber. *Opt Lett* **41**, 832–835 (2016).

144. Cusano A, Capoluongo P, Campopiano S, Cutolo A, Giordano M et al. Experimental modal analysis of an aircraft model wing by embedded fiber Bragg grating sensors. *IEEE Sens J* **6**, 67–77 (2006).

145. Moon H, Jeong J, Kang S, Kim K, Song YW et al. Fiber-Bragg-grating-based ultrathin shape sensors displaying single-channel sweeping for minimally invasive surgery. *Opt Lasers Eng* **59**, 50–55 (2014).

146. Chen Z, Wang CH, Ding ZY, Zhu DF, Guo HH et al. Demonstration of large curvature radius shape sensing using optical frequency domain reflectometry in multi-core fibers. *IEEE Photonics J* **13**, 6800809 (2021).

147. Zhao ZY, Soto MA, Tang M, Thévenaz L. Distributed shape sensing using Brillouin scattering in multi-core fibers. *Opt Express* **24**, 25211–25223 (2016).

148. Moore JP, Rogge MD. Shape sensing using multi-core fiber optic cable and parametric curve solutions. *Opt Express* **20**, 2967–2973 (2012).

149. Yi XH, Chen XY, Fan HC, Shi F, Cheng XM et al. Separation method of bending and torsion in shape sensing based on FBG sensors array. *Opt Express* **28**, 9367–9383 (2020).

150. Westbrook PS, Kremp T, Feder KS, Ko W, Monberg EM et al. Continuous multicore optical fiber grating arrays for distributed sensing applications. *J Lightwave Technol* **35**, 1248–1252 (2017).

151. Yin GL, Lu L, Zhou L, Shao C, Fu QJ et al. Distributed directional torsion sensing based on an optical frequency domain reflectometer and a helical multicore fiber. *Opt Express* **28**, 16140–16150 (2020).

152. Zeni L, Picarelli L, Avolio B, Coscetta A, Papa R et al. Brillouin optical time-domain analysis for geotechnical monitoring. *J Rock Mech Geotech Eng* **7**, 458–462 (2015).

153. Wolf A, Dostovalov A, Bronnikov K, Babin S. Arrays of fiber Bragg gratings selectively inscribed in different cores of 7-core spun optical fiber by IR femtosecond laser pulses. *Opt Express* **27**, 13978–13990 (2019).

154. Xu R, Yurkewich A, Patel RV. Curvature, torsion, and force sensing in continuum robots using helically wrapped FBG sensors. *IEEE Robot Autom Lett* **1**, 1052–1059 (2016).

155. Amantayeva A, Adilzhanova N, Issatayeva A, Blanc W,

Molardi C et al. Fiber optic distributed sensing network for shape sensing-assisted epidural needle guidance. *Biosensors* **11**, 446 (2021).

156. Jang M, Kim JS, Kang K, Kim J, Yang S. Towards finger motion capture system using FBG sensors. In *Proceedings of the 40th Annual International Conference of the IEEE Engineering in Medicine and Biology Society* 3734–3737 (IEEE, 2018); http://doi.org/10.1109/embc.2018.8513338.

157. Galloway KC, Chen Y, Templeton E, Rife B, Godage IS et al. Fiber optic shape sensing for soft robotics. *Soft Robot* **6**, 671–684 (2019).

158. Kissinger T, Chehura E, Staines SE, James SW, Tatam RP. Dynamic fiber-optic shape sensing using fiber segment interferometry. *J Lightwave Technol* **36**, 917–925 (2018).

159. Ukil A, Braendle H, Krippner P. Distributed temperature sensing: review of technology and applications. *IEEE Sens J* **12**, 885–892 (2012).

160. Adegboye MA, Fung WK, Karnik A. Recent advances in pipeline monitoring and oil leakage detection technologies: principles and approaches. *Sensors* **19**, 2548 (2019).

161. Smolen JJ. "Distributed Temperature Sensing", A DTS Primer for Oil & Gas Production. *EP2003*, **5**, 2003.

162. Nakamura S, Morooka S, Kawasaki K. Conductor temperature monitoring system in underground power transmission XLPE cable joints. *IEEE Trans Power Delivery* **7**, 1688–1697 (1992).

163. Kawai T, Takinami N, Chino T, Amano K, Watanabe K et al. A new approach to cable fault location using fiber optic technology. I. *IEEE Trans Power Delivery* **10**, 85–91 (1995).

164. Liu YP, Yin JY, Fan XZ, Wang BW. Distributed temperature detection of transformer windings with externally applied distributed optical fiber. *Appl Opt* **58**, 7962–7969 (2019).

165. Glombitza U, Hoff H. Fiber optic radar system for fire detection in cable trays. In *Proceedings of the 13th International Conference on Automatic Fire Detection* 438–459 (2004)

166. Minardo A, Catalano E, Coscetta A, Zeni G, Zhang L et al. Distributed fiber optic sensors for the monitoring of a tunnel crossing a landslide. *Remote Sens* **10**, 1291 (2018).

167. Chen XH, Zou NM, Wan YM, Ding ZW, Zhang C et al. On-line status monitoring and surrounding environment perception of an underwater cable based on the phase-locked Φ-OTDR sensing system. *Opt Express* **30**, 30312–30330 (2022).

168. Li ZQ, Zhang JW, Wang MN, Zhong YZ, Peng F. Fiber distributed acoustic sensing using convolutional long short-term memory network: a field test on high-speed railway intrusion detection. *Opt Express* **28**, 2925–2938 (2020).

169. Horiguchi T, Tateda M. Optical-fiber-attenuation investigation using stimulated Brillouin scattering between a pulse and a continuous wave. *Opt Lett* **14**, 408–410 (1989).

170. Tao W, Xu BH, He B, Du M. Research on application of distributed optical fiber sensing technology in the safety monitoring of pipeline transportation. In *Proceedings of the 2018 7th International Conference on Energy*, *Environment and Sustainable Development* 1300–1307 (Atlantis Press, 2018); http://doi.org/10.2991/iceesd-18.2018.239.

171. Liang H, Li WH, Linze N, Chen L, Bao XY. High-resolution DPP-BOTDA over 50 km LEAF using return-to-zero coded pulses. *Opt Lett* **35**, 1503–1505 (2010).

172. He ZY, Liu QW. Optical fiber distributed acoustic sensors: a review. *J Lightwave Technol* **39**, 3671–3686 (2021).

173. Tejedor J, Macias-Guarasa J, Martins HF, Pastor-Graells J, Corredera P et al. Machine learning methods for pipeline surveillance systems based on distributed acoustic sensing: a review. *Appl Sci* **7**, 841 (2017).

174. Dou S, Lindsey N, Wagner AM, Daley TM, Freifeld B et al. Distributed acoustic sensing for seismic monitoring of the near surface: a traffic-noise interferometry case study. *Sci Rep* **7**, 11620 (2017).

175. Walter F, Gräff D, Lindner F, Paitz P, Köpfli M et al. Distributed acoustic sensing of microseismic sources and wave propagation in glaciated terrain. *Nat Commun* **11**, 2436 (2020).

176. Liu T, Li H, He T, Fan CZ, Yan ZJ et al. Ultra-high resolution strain sensor network assisted with an LS-SVM based hysteresis model. *Opto-Electron Adv* **4**, 200037 (2021).

177. Lellouch A, Lindsey NJ, Ellsworth WL, Biondi BL. Comparison between distributed acoustic sensing and geophones: downhole microseismic monitoring of the FORGE geothermal experiment. *Seismol Res Lett* **91**, 3256–3268 (2020).

178. Sun QZ, Liu DM, Xia L, Wang J, Liu HR et al. Experimental demonstration of multipoint temperature warning sensor using a multichannel matched fiber Bragg grating. *IEEE Photonics Technol Lett* **20**, 933–935 (2008).

179. Zhang W, Yan ZJ, Sun QZ. Multichannel fiber Bragg grating for distributed sensing with high spatial resolution. *Proc SPIE* **10849**, 1084919 (2018).

180. Sanders GA, Szafraniec B, Liu RY, Laskoskie CL, Strandjord LK et al. Fiber optic gyros for space, marine, and aviation applications. *Proc SPIE* **2837**, 61–71 (1996).

181. Bergh RA, Lefevre HC, Shaw HJ. All-single-mode fiber-optic gyroscope. *Opt Lett* **6**, 198–200 (1981).

182. Bohnert K, Gabus P, Kostovic J, Brändle H. Optical fiber sensors for the electric power industry. *Opt Lasers Eng* **43**, 511–526 (2005).

183. Liu C, Lü JW, Liu W, Wang FM, Chu PK. Overview of refractive index sensors comprising photonic crystal fibers based on the surface plasmon resonance effect [Invited]. *Chin Opt Lett* **19**, 102202 (2021).

184. Sharma AK, Pandey AK, Kaur B. A Review of advancements (2007–2017) in plasmonics-based optical fiber sensors. *Opt Fiber Technol* **43**, 20–34 (2018).

185. Keiser G. *Biophotonics*: *Concepts to Applications* (Springer, Singapore, 2016).

186. Pan T, Lu DY, Xin HB, Li BJ. Biophotonic probes for bio-detection and imaging. *Light Sci Appl* **10**, 124 (2021).

187. Soares MS, Vidal M, Santos NF, Costa FM, Marques C et al. Immunosensing based on optical fiber technology: recent advances. *Biosensors* **11**, 305 (2021).

188. Miao YS, Jing JC, Desai V, Mahon SB, Brenner M et al. Automated 3D segmentation of methyl isocyanate-exposed rat trachea using an ultra-thin, fully fiber optic optical coherence endoscopic probe. *Sci Rep* **8**, 8713 (2018).

189. Tan ACS, Tan GS, Denniston AK, Keane PA, Ang M et al. An overview of the clinical applications of optical coherence tomography angiography. *Eye* **32**, 262–286 (2018).

190. Song G, Jelly ET, Chu KK, Kendall WY, Wax A. A review of low-cost and portable optical coherence tomography. *Prog Biomed Eng* **3**, 032002 (2021).

191. Kwak J, Lee W, Kim JB, Bae SI, Jeong KH. Fiber-optic plasmonic probe with nanogap-rich Au nanoislands for on-site surface-enhanced Raman spectroscopy using repeated solid-state dewetting. *J Biomed Opt* **24**, 037001 (2019).

192. Xi X, Liang CY. Perspective of future SERS clinical application based on current status of raman spectroscopy clinical trials. *Front Chem* **9**, 665841 (2021).

193. Langer J, de Aberasturi DJ, Aizpurua J, Alvarez-Puebla RA, Auguié B et al. Present and future of surface-enhanced raman scattering. *ACS Nano* **14**, 28–117 (2020).

194. Zeni L, Perri C, Cennamo N, Arcadio F, D'agostino G et al. A portable optical-fibre-based surface plasmon resonance biosensor for the detection of therapeutic antibodies in human serum. *Sci Rep* **10**, 11154 (2020).

195. Zhu SD, Xie ZM, Chen YZ, Liu SY, Kwan YW et al. Real-time detection of circulating tumor cells in bloodstream using plasmonic fiber sensors. *Biosensors* **12**, 968 (2022).

196. Yu X, Zhang SY, Olivo M, Li NX. Micro- and nano-fiber probes for optical sensing, imaging, and stimulation in biomedical applications. *Photonics Res* **8**, 1703–1724 (2020).

197. Hu DJJ, Lim JL, Jiang M, Wang YX, Luan F et al. Long period grating cascaded to photonic crystal fiber modal interferometer for simultaneous measurement of temperature and refractive index. *Opt Lett* **37**, 2283–2285 (2012).

198. Xu ZL, Lim J, Hu DJJ, Sun QZ, Wong RYN et al. Investigation of temperature sensing characteristics in selectively infiltrated photonic crystal fiber. *Opt Express* **24**, 1699–1707 (2016).

199. Kaushik S, Tiwari UK, Deep A, Sinha RK. Two-dimensional transition metal dichalcogenides assisted biofunctionalized optical fiber SPR biosensor for efficient and rapid detection of bovine serum albumin. *Sci Rep* **9**, 6987 (2019).

200. Dinish US, Balasundaram G, Chang YT, Olivo M. Sensitive multiplex detection of serological liver cancer biomarkers using SERS-active photonic crystal fiber probe. *J Biophoton* **7**, 956–965 (2014).

201. Yan H, Liu J, Yang CX, Jin GF, Gu C et al. Novel index-guided photonic crystal fiber surface-enhanced Raman scattering probe. *Opt Express* **16**, 8300–8305 (2008).

202. Xie Z, Lu Y, Wei H, Yan J, Wang P et al. Broad spectral photonic crystal fiber surface enhanced Raman scattering probe. *Appl Phys B* **95**, 751–755 (2009).

203. Gong TX, Zhang N, Kong KV, Goh D, Ying C et al. Rapid SERS monitoring of lipid-peroxidation-derived protein modifications in cells using photonic crystal fiber sensor. *J Biophoton* **9**, 32–37 (2016).

204. Gong TX, Cui Y, Goh D, Voon KK, Shum PP et al. Highly sensitive SERS detection and quantification of sialic acid on single cell using photonic-crystal fiber with gold nanoparticles. *Biosens Bioelectron* **64**, 227–233 (2015).

205. He ZY, Wang P, Ye XS. Novel endoscopic optical diagnostic technologies in medical trial research: recent advancements and future prospects. *Biomed Eng Online* **20**, 5 (2021).

206. Gora MJ, Suter MJ, Tearney GJ, Li XD. Endoscopic optical coherence tomography: technologies and clinical applications [Invited]. *Biomed Opt Express* **8**, 2405–2444 (2017).

207. Lu LD, Yong MC, Wang QS, Bu XD, Gao QH. A hybrid distributed optical fiber vibration and temperature sensor based on optical Rayleigh and Raman scattering. *Opt Commun* **529**, 129096 (2023).

Acknowledgements

Author contributions

H. H. Liu and D. J. J. Hu contributed equally to this work in drafting the manuscript, Q. Z. Sun contributed to review on wearable sensor and shape sensing; L. Wei and K. W. Li contributed to review and prospects on multimaterial multifunctional fiber; C. R. Liao, B. Z. Li, and C. Zhao contributed to review and prospects on lab in/on a fiber; X. Y. Dong and Y. H. Tang contributed to review of general sensing applications; Y. H. Xiao contributed to review of industrial application; G. Keiser contributed to review of biomedical sensing; P. P. Shum supervised the review. All authors contributed to revision on the manuscript.

Competing interests

The authors declare no competing financial interests.